

IMPACT-TYPE VIBRATION EFFECTS ON YOUNG CONCRETE FOR TUNNELLING

Lamis Ahmed

IMPACT-TYPE VIBRATION EFFECTS ON YOUNG CONCRETE FOR TUNNELLING

**Effekter från vibrationar av stöttyp på ung betong
för tunnlrar**

Lamis Ahmed, KTH

Preface

Rock construction in the Scandinavian countries are traditionally carried out by blasting and the rock support by shotcrete and bolts. The rock support is normally applied after each blast round. The support shotcrete needs a certain waiting time before the following blast can be initiated which affects the productivity. Fresh concrete is affected by vibrations from blasting, but there is still limited knowledge about the necessary waiting time and distance to blasting. In practice, a conservative approach with extensive margins will result in longer construction time and higher costs for projects than necessary. Other vibration sources in the construction industry are also relevant and included in the research report, these sources are traffic, different types of heavy machinery and from piling.

Previous literature studies show that limits for vibrations near concrete structures are unnecessary low. The research at the Royal Institute of Technology (KTH) within this field was previously carried out using laboratory tests and non-complex numerical modelling. In the present research project the numerical modelling is developed further using finite elements modelling with dynamic analyses. Here the rock material, the shotcrete and the interface between these materials is included in the analyses. Thereafter, the results have been checked against actual data from different types of tunnels. The result from the present research project describe the effect of vibrations on young concrete and also a comparison between shotcrete and concrete.

This research project was performed at KTH by Ph.D. Lamis Ahmed together with a working group consisting of Professor Anders Ansell and Ph.D. Richard Malm. A reference group consisting of Thomas Dalmalm (Swedish Transport Administration), Nils Rydén (Lund University/Peab), Hans Hedlund (Luleå Technical University/Skanska), Johan Silfwerbrand (KTH) and Per Tengborg (BeFo). The project was funded by BeFo (Rock Engineering Research Foundation) together with SBUF.

Stockholm in November 2016

Per Tengborg

Förord

Bergbyggande i Skandinavien utförs i huvudsakligen genom sprängning och berget förstärks då oftast med bultar och sprutbetong efter en sprängsalva. Nästa sprängning vill man skjuta snarast möjligt för att minska väntetider och hålla en god produktivitet. Färsk sprutbetong påverkas av vibrationer, t ex från sprängning, men kunskapen är begränsad kring vilka väntetider och avstånd som behövs. I praktiken innebär ett konservativt synsätt med för stora marginaler att bergbyggandsprojekt tar längre tid och byggs till högre kostnad än nödvändigt. Vibrationer från andra källor i byggsammanhang än sprängning är också relevanta, främst från trafik, olika typer av tunga maskiner och pålning, och innefattas i den presenterade forskningsrapporten.

Tidigare litteraturstudier visar att de gränsvärden för vibrationer som används nära betongkonstruktioner är onödigt låga. Forskningen vid KTH har tidigare utförts med praktiska försök i laboratorium och enklare numerisk modellering, men i föreliggande forskningsprojekt går man vidare och utför numeriska beräkningar med finita elementmodeller i en dynamiska analys. Här ingår bergmassan, sprutbetong och gränsskiktet däremellan. Därefter har resultaten stämts av mot verkliga försök i gruvorter och tunnlar. Resultatet av forskningsprojektet beskriver påverkan av vibrationer på ung betong och även jämförelse mellan sprutbetong och gjuten betong.

Forskningsprojektet utfördes av Teknologie Doktor Lamis Ahmed tillsammans med en arbetsgrupp bestående av Professor Anders Ansell och Teknologie Doktor Richard Malm, samtliga KTH Byggvetenskap, avd Betongbyggnad. En referensgrupp bestående av Thomas Dalmalm (Trafikverket), Nils Rydén (Lunds Universitet/Peab), Hans Hedlund (Luleå Tekniska Universitet/Skanska), Johan Silfwerbrand (KTH Byggvetenskap) och Per Tengborg (BeFo) har bidragit med synpunkter under projektets gång. Projektet finansierades av BeFo (Stiftelsen Bergteknisk Forskning) tillsammans med SBUF.

Stockholm i november 2016

Per Tengborg

Summary

The strive for a time-efficient construction process naturally put focus on the possibility of reducing the time of waiting between stages of construction, thereby minimizing the construction cost. If recently placed concrete, cast or sprayed, is exposed to impact vibrations at an early age while still in the process of hardening, damage that threatens the function of the hard concrete may occur. A waiting time when the concrete remains undisturbed, or a safe distance to the vibration source, is therefore needed. However, there is little, or no, fully proven knowledge of the length of this distance or time and there are no established guidelines for practical use. Therefore, conservative vibration limits are used for young and hardening concrete exposed to vibrations from e.g. blasting.

As a first step in the dynamic analysis of a structure, the dynamic loads should always be identified and characterized. Here it is concluded that impact-type loads are the most dangerous of possible dynamic loads on young and hardening concrete. Shotcrete (sprayed concrete) on hard rock exposed to blasting and cast laboratory specimens subjected to direct mechanical impact loads have been investigated using finite element models based on the same analysis principles. Stress wave propagation is described in the same way whether it is through hard rock towards a shotcrete lining or through an element of young concrete.

Within this project, work on evaluating and proposing analytical models are made in several steps, first with a focus on describing the behaviour of shotcrete on hard rock. It is demonstrated that wave propagation through rock towards shotcrete can be described using two-dimensional elastic finite element models in a dynamic analysis. The models must include the material properties of the rock and the accuracy of these parameters will greatly affect the results. It is possible to follow the propagation of stress waves through the rock mass, from the centre of blasting to the reflection at the shotcrete-rock interface. It is acceptable to use elastic material formulations until the strains are outside the elastic range, which thus indicates imminent material failure. Comparisons are made between numerical results and measurements from experiments in mining tunnels with ejected rock mass and shotcrete bond failure, and with measurements made during blasting for tunnel construction where rock and shotcrete remained intact. The calculated results are in good correspondence with the in situ observations and measurements, and with previous numerical modelling results. Examples of preliminary recommendations for practical use are given and it is demonstrated how the developed models and suggested analytical technique can be used for further detailed investigations.

Keywords: Young concrete · Shotcrete · Rock · Impact-type vibration · Finite element method · Fracture mechanics model · Crack width

Sammanfattning

Strävan efter en tidseffektiv byggprocess fokuserar på ett naturligt sätt på möjligheten att minska väntetiderna mellan byggetapper, vilket minimerar byggkostnaden. Om nyligen placerad betong, gjuten eller sprutad, utsätts för vibrationer av stöttyp vid tidig ålder då härdningsprocessen fortfarande pågår, finns risk för skador som hotar att försämra funktionen hos den fullhårdnade betongen. Därför behövs en väntetid där betongen förblir ostörd, eller ett säkert avstånd till vibrationskällan. Det finns däremot liten eller ingen fullt vedertagen kunskap om längden på detta avstånd, eller tidsperiod, och det finns heller inga fastställda riktlinjer för praktisk användning. Därför används idag konservativa gränsvärden för ung och hårdnande betong som utsätts för vibrationer från t.ex. sprängning.

Inom detta projekt genomförs arbetet med att utvärdera och föreslå analysmodeller i flera steg, först med fokus på att beskriva beteendet hos sprutbetong på hårt berg. Det visas att vågutbredning genom berget mot sprutbetongen kan beskrivas med hjälp av tvådimensionella elastiska finita elementmodeller i en dynamisk analys. Modellerna måste inkludera bergmaterialets egenskaper och riktigheten hos dessa parametrar kommer att ha stor påverkan på resultaten. Det är möjligt att följa utbredningen av spänningsvågor genom bergmassan, från sprängningens centrum till reflektion vid gränsskiktet mellan sprutbetong och berg. Tillräcklig noggrannhet ges med elastiska materialformuleringar, tills töjningar överskrider det elastiska området vilket indikerar förestående materialbrott. Den högre komplexiteten hos denna typ av modell, jämfört med mekaniska modeller med massor och fjäderelement, kommer att möjliggöra analyser med avancerade geometrier. Jämförelser görs här mellan numeriska resultat och mätningar från experiment i gruvtunnlar, med utstött bergmassa och vidhäftningsbrott, och med mätningar gjorda under sprängning för tunnelbygge, där berg och sprutbetong förblev intakta. De beräknade resultaten är i god överensstämmelse med fältförsöken och med tidigare presenterade numeriska resultat. Exempel på preliminära rekommendationer för praktiskt bruk ges och det visas hur föreslagen analysteknik och de utvecklade modellerna kan användas för kommande detaljerade undersökningar.

Nyckelord: Ung betong · Sprutbetong · Berg · Stötar och vibrationer · Finita elementmetoden · Brottmekanisk modell · Sprickbredd

Contents

| | |
|-------------------------------------------------------|------------|
| Summary | v |
| Sammanfattning | vii |
| 1 Introduction..... | 1 |
| 1.1 Background | 1 |
| 1.2 Early age concrete | 2 |
| 1.3 Shotcrete | 3 |
| 1.4 Previous research..... | 4 |
| 1.5 Current research project | 9 |
| 2 Impact-type vibrations | 11 |
| 2.1 Dynamic load types | 11 |
| 2.2 Traffic vibrations | 14 |
| 2.3 Machine vibrations and pile-driving | 15 |
| 2.4 Blasting..... | 16 |
| 3 Finite element analysis..... | 19 |
| 3.1 Finite element models | 19 |
| 3.2 In-situ case..... | 22 |
| 4 Numerical results | 25 |
| 4.1 Tunnel profile and plane | 25 |
| 4.2 In-situ case | 31 |
| 5 Impact vibration limits and guidelines | 35 |
| 5.1 Standards and specifications | 35 |
| 5.2 Young concrete vibration limits | 36 |
| 5.3 Shotcrete vibration limits | 38 |

| | | |
|----------|----------------------------------------------|-----------|
| 6 | Recommendations and conclusions | 41 |
| 6.1 | Load type | 41 |
| 6.2 | Test results and measurement..... | 42 |
| 6.3 | Concrete and shotcrete | 42 |
| | Bibliography | 45 |

Chapter 1

Introduction

A criterion for how severe impact induced vibrations that can be allowed to reach young and hardening concrete is needed for efficient civil engineering projects, e.g. casting of concrete foundations on ground, tunnelling or other underground constructions. Striving for a more time-efficient construction process naturally focuses on the possibilities of reducing the times of waiting between stages of construction, which will lead to a reduced construction cost.

1.1 Background

Recently placed, young and hardening concrete is vulnerable to high intensity vibrations of impact-type that may cause a reduction of its strength in the hardened state. Vibration stress waves will propagate through a concrete volume and depending on the existence of free and restrained boundary surfaces, compressive and tensile stresses will appear. Since the compressive strength of concrete is higher than the tensile strength, damage due to tensile cracking of the concrete matrix may occur during the hardening process. The damaging mechanisms inside curing concrete subjected to impact-type vibrations are complicated and little is known about their effects. Therefore, conservative vibration limits have been used for hardening concrete exposed to vibrations, in many cases leaving engineers to conduct empirical investigations and testing without any clear and reliable guidelines given. This is reflected in the differences that exist between limits specified in different national standards and handbooks, often given with allowed peak particle velocity (PPV) at a certain point where damage protection is required.

The allowable PPV levels vary strongly as the concrete hardens and its strength increases. Also, the maximum PPV that can be allowed close to recently placed concrete depends on geometry, construction type, and load situation and may be fundamentally different if e.g. mass concrete or shotcrete (sprayed concrete) is studied. The damage caused in shotcrete on rock is often the result of bond failure while damage on aboveground concrete structures from e.g. underground blasting is due to structural dynamic response problems. Therefore, it is necessary to determine reliable safety limits for impact vibration in relation to concrete type, concrete ages, dynamic characteristics, etc. However, to establish reliable guidelines comparison between in situ or laboratory observations and measurements with finite element modelling results are needed to gain the understanding of the causes of possible damage in young concrete exposed to severe vibrations.

1.2 Early age concrete

There are several alternative definitions of ‘*early age concrete*’, used differently within the various fields of concrete engineering and research. A review of common terms and their corresponding time spans is presented by Ansell and Silfwerbrand [12], here summarized in Table 1.1. The term ‘*young concrete*’ often refers to recently placed concrete, being 0–12 hours old while ‘*old concrete*’ is concrete older than one week. For ages between young and old, the term ‘*intermediate age concrete*’ is used. With reference to the hardening process, ‘*initial setting*’ corresponds to the time when concrete is no longer workable and has very little or no slump while ‘*final setting*’ indicates the time at which the concrete begins to harden, but when still no measurable strength can be observed, [46]. The American Concrete Institute [1] defines ‘*early age of concrete*’ as the period after final setting during which properties are changing rapidly. This definition is similar to that for ‘*green concrete*’, defined as concrete that has undergone final setting but not fully hardened. These two definitions imply that the concrete has reached final set but has not gained much strength. The early strength of concrete or mortar is usually [1] given at various times during the first 72 hours after placement, for ‘*early age concrete*’ often defined as concrete between setting and approximately 24–72 hours old, [26]. Research findings indicate that the setting period represents the interval of the most rapid hydration, followed by a period of reduced hydration activity, i.e. induction. The beginning of the setting period is not mainly defined since it depends on many factors, i.e. type of cement, water/cement ratio, temperature, etc. However, e.g. the Swedish Concrete handbook [57] states that the setting period starts after 3–5 hours from the first contact between water and cement. Through the setting period, a major portion of the cement hydrates and then solidifies which normally continues up to 24–72 hours. In the present study, ‘*early age concrete*’ is used to denote concrete less than 72 hours old. For very early ages the term ‘*young concrete*’ is used, which here represents the period from first contact between cement and water up to 12 hours of age. The most critical concrete age is often assumed to be within 3–14 hours after casting, but is believed to vary with the type of concrete and curing conditions, see [12 and 32].

Table 1.1: A compilation of terminology for young and early age concrete, from [12].

En sammanställning av terminologi för betong, vid ung och tidig ålder, från [12]

| Term | Concrete ages | Definition given by: |
|---------------------------|-----------------------------------|--------------------------|
| Fresh concrete | concrete before setting | Byfors [26] |
| Green concrete | freshly placed, ≤ 24 hours | Hulshizer and Desai [31] |
| Young concrete | 0–12 hours | Akins and Dixon [10] |
| Early age concrete | between setting and app. 1–3 days | Byfors [26] |
| Intermediate age concrete | 12 hours – 7 days | Akins and Dixon [10] |
| Almost hardened concrete | app. 1–3 days to 28 days | Byfors [26] |
| Old concrete | ≥ 7 days | Akins and Dixon [10] |
| Hardened concrete | ≥ 28 days | Byfors [26] |

1.3 Shotcrete

Shotcrete is concrete projected pneumatically onto a surface, using either the dry mix or the wet mix method. The latter has been widely used for tunnelling work in hard rock and its flexibility in the choice of application thickness, material compositions (e.g., fibre content), output capacity and fast early strength development makes shotcrete a material well suited for rock support. Most construction work in underground rock involves the use of explosives for excavation work. Rock surfaces are often secured with shotcrete immediately after the excavation blasting to prevent fallout of smaller blocks. Therefore, shotcrete must often be able to carry loads and withstand disturbances early after spraying, [25]. However, movements in the rock mass and especially vibrations from blasting during tunnelling may cause damage that threatens the performance of the hardened shotcrete. Damage may lead to full or partial debonding between shotcrete and rock that could affect the efficiency of the rock support and the overall safety of e.g. a tunnel or underground opening. The relation between the strength growth for important material parameters such as modulus of elasticity and tensile strength is important for the capacity to resist vibrations, [25]. Material data for cast concrete is often used for analyses involving shotcrete. However, even though the basic material compositions are similar, the method of placement, the use of set accelerators and other additives gives shotcrete unique material properties. The underground temperatures and humidity also affect the strength growth ratio that differs from that of cast concrete.

In tunnelling, the use of shotcrete is often restricted near the area where blasting takes place, due to the risk of vibration damage, as demonstrated in Figure 1.1. An important example is the driving of two parallel tunnels that requires coordination between the two excavations so that blasting in one tunnel does not, through vibrations, damage temporary support systems in the other tunnel prior to installation of a robust, permanent support, see Figure 1.2. Similar problems also arise in mining where the grid of drifts in a modern mine is dense. This means that supporting systems in one drift are likely to be affected by vibrations in a neighbouring drift. Thus, to be able to excavate as much ore volume as possible, there is a need to know how close, in time and distance, to shotcrete blasting can be allowed. Previous studies show that shotcrete without reinforcement, also as young as a couple of hours, can withstand vibration levels as high as 500–1000 mm/s while sections with loss of bond and ejected rock appear for vibration velocities higher than 1000 mm/s [13]. Similar measurements, based on in situ experiments conducted in Japan [45], showed that vibration velocities of 700 mm/s cracked the observed shotcrete lining. The response of steel fibre-reinforced and steel mesh-reinforced shotcrete linings subjected to blasts was investigated in a Canadian mine [59]. It was observed that the shotcrete remained attached to the rock surface for vibration levels up to 1500–2000 mm/s, with only partial cracking observed in the shotcrete.

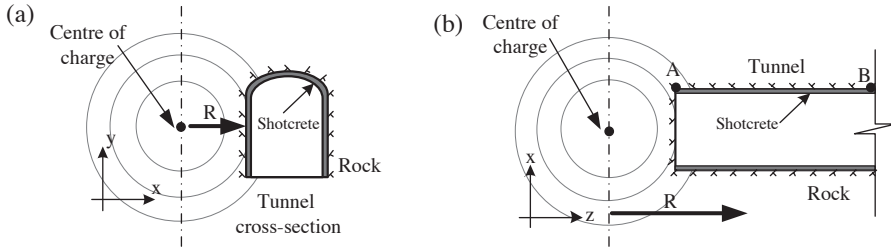


Figure 1.1: Examples of stress waves in rock;(a)tunnel profile and (b)tunnel plane, from [8].

Exempel på spänningstågor i berg; (a) tunnelprofil och (b) tunnelplan, från [8].

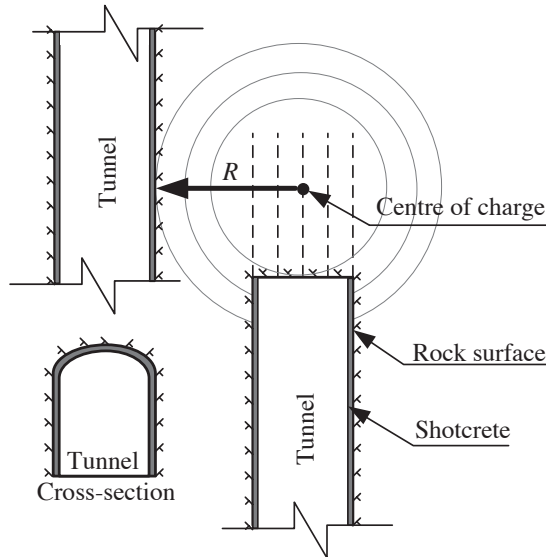


Figure 1.2: Construction of two parallel tunnels, redrawn from [35].

Byggande av två parallella tunnlar, omritad från [35].

1.4 Previous research

As a first step towards understanding of the vibration resistance of young shotcrete, in situ tests were conducted in a Swedish mine, [17]. The tests were conducted with sections of plain, unreinforced shotcrete projected on tunnel walls and exposed to vibrations from explosive charges detonated inside the rock, at ages of 1 to 25 hours, as shown in Figure 1.3. The response of the rock was measured with accelerometers mounted on the rock surface and inside the rock. The tests indicated that the major failure mechanism is sudden de-bonding at the rock–shotcrete interface. It was concluded that shotcrete without reinforcement, also as young as a couple of hours, can withstand vibration levels as high as 500–1000 mm/s while section with loss of bond and ejected rock were found for vibration velocities higher than 1000 mm/s. The results also

provided information about stress wave propagation in hard rock, and a scaling relation for PPV as function of distance and explosive charge weight. The observed particle velocities in rock will show a decrease in magnitude with increasing distance R to the source of explosion. This decay is caused by geometrical spreading and hysteretic damping in the rock [21]. To predict peak particle velocity in the rock mass, functions of the scaled distance to the explosive charge are often used. In this study, the square-root scaling is employed to predict the attenuation or decay of PPV. Thus, and based on regression analysis from in-situ results [13], the PPV is governed by:

$$v_{\max} = 700 \left(\frac{R}{\sqrt{Q}} \right)^{-1.5} \quad (\text{mm/s}) \quad (1.1)$$

where v_{\max} is the maximum PPV at a distance R from the point charge gives the relation between PPV, R (in meter) and Q is the weight of the explosives (in kg).

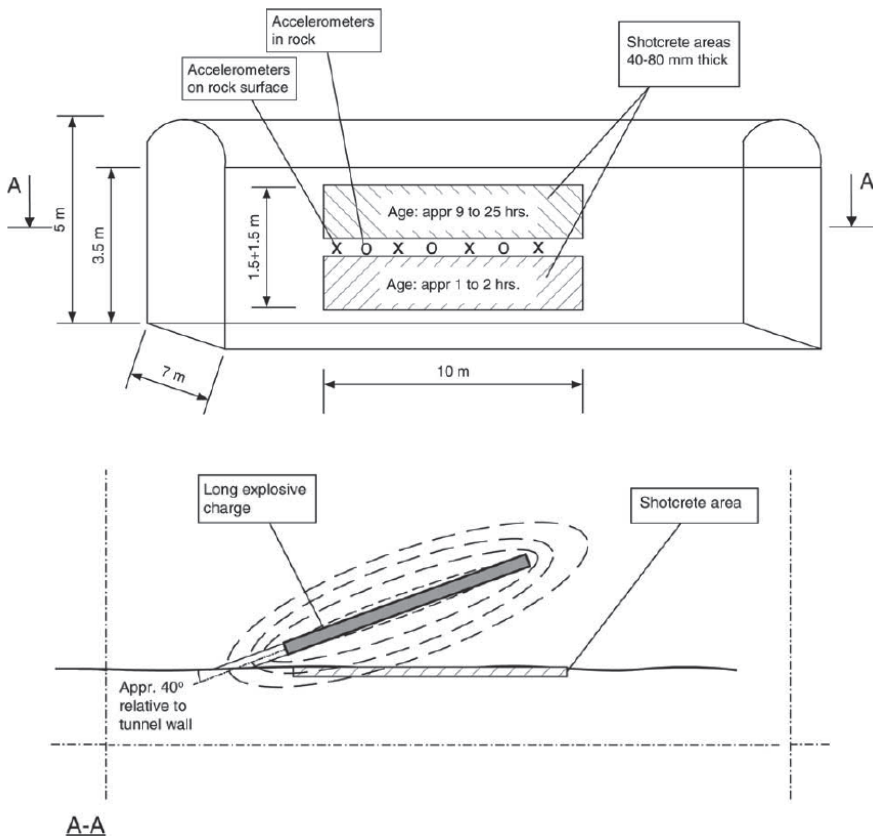


Figure 1.3: Schematic view of a test site. Explosive charge in rock behind shotcrete areas, from [17]. *Skiss av en provplats. Sprängladdning i berg bakom betongsprutade områden, från [17].*

Another attempt to characterize the vibrations that occur along tunnel walls during excavation blasting has been performed by Reidarman and Nyberg [51]. The measurements were done during construction of the Southern Link (Södra länken) road tunnel system in Stockholm, Sweden. The accelerometers used were positioned following the same system as for the Kiirunavaara measurements, described above. The results from this investigation are well suited for evaluation of finite element (FE) models. No shotcrete damage was observed following the blasting, due to the very restrict guidelines used, and it can thus be assumed that the shotcrete-rock system behaves elastically throughout the passage of the stress waves. The measurement of vibrations from four blasting rounds was done using accelerometers located along an axis stretching approximately 5-50 m behind the tunnel front. Accelerations were measured in two directions, parallel with and perpendicular to the tunnel walls, recorded and later numerically recalculated into corresponding velocity-time records. All measurement points were situated 300 mm into the rock. The layout of the test tunnel with the position for the measurement points is shown in Figure 1.4. It should be noted that the advancement of the tunnel front is towards the left in the figure and that each blasting round results in 5 m new tunnel length, except for the third round which gave a 10 m extension. The figure also shows how some measurement points were abandoned in favour of new points closer to the tunnel face, thus approximately giving equal spacing between the points for each of the four rounds.

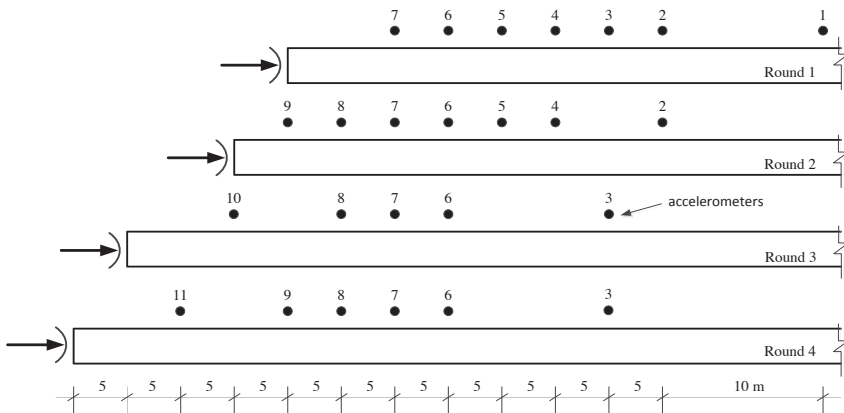


Figure 1.4: Tunnel with advancing front during four excavations rounds. Test layout with positions of measurement points, from [6].

Tunnel med propageranda front under fyra utgrävningsssteg. Försöksplan med positioner för mätpunkter, från [6].

The maximum velocities for each point vs. the distances along the tunnel wall are shown in Figure 1.5, with curves fitted using the method of least squares, in the direction parallel with and perpendicular to the tunnel wall $v_{\max,x}$ and $v_{\max,y}$, respectively, giving:

$$\begin{cases} v_{\max,x} = 74.81e^{-0.065x} \text{ (mm/s)} \\ v_{\max,y} = 18.48e^{-0.026x} \text{ (mm/s)} \end{cases} \quad (1.2)$$

with the distance x along the tunnel given in metres. It should be noted that the ppv from a single blast hole did not exceed 80 mm/s in any test point, in any direction.

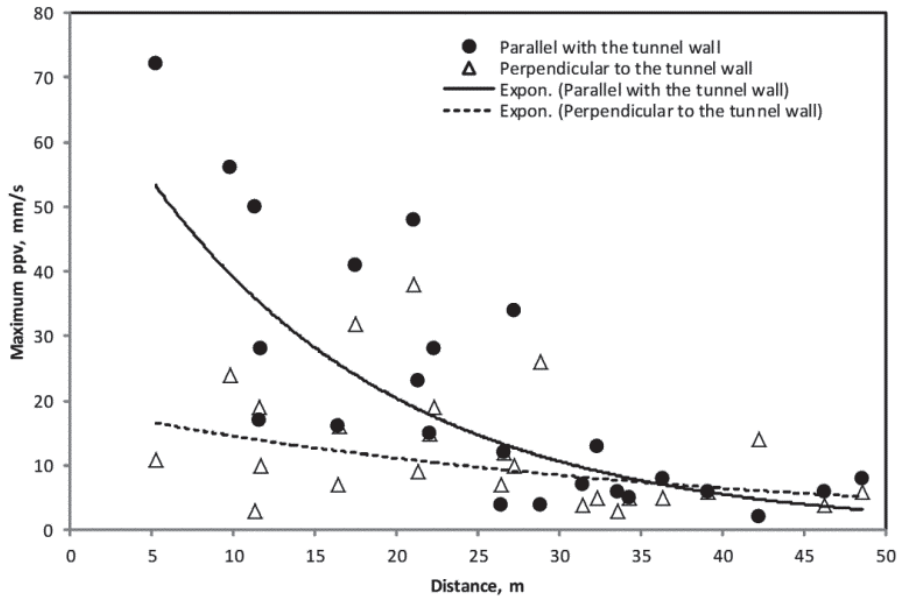


Figure 1.5: Maximum PPV versus distance along the tunnel wall, from [6].

Maximal PPV mot avstånd längs tunnelns vägg, från [6].

These values should be compared with the observed damage limits for shotcrete on rock, here compiled in Table 1.1. The results have also been used as input data and for verification in analytical and numerical studies during previous projects [16, 18-19], and within the current project, see [2, 4-5 and 8].

The in-situ tests conducted underground in a Swedish mine [17] were evaluated using comparisons with results from numerical models [16, 18-19]. These were based on elastic stress wave theory and structural dynamics and with relatively small computational effort made it possible to compare a large number of calculations with various combinations of input data. The previously used engineering models were compared and evaluated through calculations and comparisons with existing data [8]. Results from a non-destructive laboratory experiment were also used to provide test data for the models [7]. A more sophisticated, dynamic finite element model was also developed and tested using the numerical program Abaqus [54]. This allows modelling of more complex geometries and provides more detailed analysis results.

Table 1.1: Vibration velocities PPV when shotcrete damage occurs based on in situ measurements, from [3].

Vibrationshastigheter PPV när sprutbetong skador sker baserat på mätningar på plats, från [3].

| | PPV at damage, mm/s | Comments: |
|--------------------------|---------------------|------------------------|
| Kiirunavaara tests [17] | 500–1000 | Young shotcrete |
| Japanese tunnelling [45] | 700–1450 | |
| Mining, full scale [36] | app. 1000–1800 | |
| Canadian tests [59] | 1500–2000 | Steel fibre reinforced |

On the other hand, there are often practical problems associated with testing of young and hardening concrete. Material properties such as compressive strength, tensile strength and modulus of elasticity are difficult to measure on concrete younger than 12 hours. For younger concrete it may be difficult to remove casting moulds for stiffness or strength measurement, [38]. Despite this, the effects of vibration on early age concrete have been studied through a number of tests carried out using widely different methods. A variety of methods for applying vibration loads to concrete test specimens has been used. These vary from hammering the specimens to produce impact vibration, or vibrating the specimens on a shaker table, to subjecting the specimens to ground vibrations at a construction site. The latter is often done by placing concrete specimens adjacent to sources of construction-induced vibration such as rock-blasting, pile-driving, heavy traffic, or machine vibrations, as further explained in [2]. There is no agreement on how vibration damage to the concrete should be defined and detected. Measurement of only the compressive strength of vibration-exposed and later hardened concrete specimens might not reveal the full effects of the shock vibration applied [39]. There might also be difficulties in detecting damage from vibrations in early age concrete since e.g. hairline cracks are difficult to observe with the naked eye. However, early investigations such as the study by Esteves [28], relied on visual inspection to detect surface cracks as a sign of vibration damage to the concrete, [27]. Due to this, large variations in the results between experimental studies can be seen demonstrating that more clear failure criteria such as reduction in compressive or tensile strength should be used. The vibration resistance of concrete depends more on tensile than on compressive strength, and vibration damages also show mainly in the form of cracking and reduction in tensile strength, [38]. However, because tensile strength is more difficult to test than compressive strength, especially for young concrete, many researchers therefore omitted to investigate the tensile strength. One reason is that reinforced concrete is often designed in the cracked state making tensile strength less important with respect to impact vibrations in such cases, see e.g. Hulshizer and Desai [31]. Thus, due to the lack of detailed knowledge of how vibrations cause damage to early age concrete there are no generally accepted methods for estimating these limits. In some tests, despite shock vibrations up to what was believed to be a very high PPV, no damage to the concrete specimens had been detected. In most of these tests, the threshold vibration intensity that would cause vibration damage had not yet been reached and the results obtained were only safe PPV levels that would not cause vibration damage, and no ultimate vibration limits. Although the tensile strength is relatively low during the first 24 hours after casting, it has been suggested that within the first 2 hours, i.e. before initial set, young concrete is able to withstand PPV up to 100 mm/s, [31 and 48], and may also benefit from the re-vibration [12].

1.5 Current research project

This report is a summary of a PhD thesis which investigates finite element models for shotcrete exposed to impact-type loads [9]. The project aimed at suggesting numerical methods suitable for analysis of young and hardening concrete subjected to impact-type vibrations. Focus is on how impact-type vibrations damage young concrete and when impact is the most relevant load case. One important research question is how to perform a dynamic analysis that realistically captures the characteristics of the load, the structural response of the analysed concrete element or volume and indicates concrete damage caused by the load. The project is a continuation from previous investigations of the effect on young shotcrete from blasting vibrations. The first project phase has also been presented in a licentiate thesis [8] and its appended papers, here also included as [2, 4-5], on models for analysis of shotcrete on rock exposed to blasting. The previously used engineering models were evaluated through calculations and comparisons with existing data. Results from a non-destructive laboratory experiment were also used to provide test data for the models. A more sophisticated, dynamic finite element model was also developed and tested using the numerical program Abaqus [54]. This allows modelling of more complex geometries and provides more detailed analysis results. The second phase, summarized here together with the conclusions from the first part of the project, also studied the effect from vibrations on young and hardening cast concrete. The developed and tested finite element model was also used with a non-linear material formulation that can simulate concrete cracking, for more details see [3 and 9]. The case with shotcrete on hard rock is thus a special case that can be analysed with similar methods as cast concrete elements and volumes, but for other geometries and material properties. The most important difference is here the failure modes, where cast concrete develops cracks while shotcrete often fails due to loss of bond to the rock. For more detailed information, see the thesis [9] and its appended papers [2-6, 11].

The PhD thesis is based on work contained in the following articles:

- Ansell A, Ahmed L. Impact load vibrations on young concrete. Submitted to *Structural Concrete*, 2015.
- Ahmed L, Ansell A. Laboratory investigation of stress waves in young shotcrete on rock. *Magazine of Concrete Research* 64(10):899-908, 2012.
- Ahmed L, Ansell A. Structural dynamic and stress wave models for the analysis of shotcrete on rock exposed to blasting. *Engineering structures* 35:11-17, 2012.
- Ahmed L, Ansell A, Malm R. Finite element simulation of shotcrete exposed to underground explosions. *Nordic Concrete Research* 45:59-74, 2012.
- Ahmed L, Ansell A. Vibration vulnerability of shotcrete on tunnel walls during construction blasting. *Tunnelling and Underground Space Technology* 42:105–111, 2014.
- Ahmed L, Ansell A, Malm R. Numerical modelling and evaluation of laboratory tests with impact loaded young concrete prisms. Submitted to *Materials and Structures*, 2015.

As complement to the above, the following additional publications also present results from the project:

- Ahmed L. Models for analysis of young cast and sprayed concrete subjected to impact-type loads. Doctorate thesis. Stockholm: KTH Royal Institute of Technology; 2015.
- Ahmed L. Models for analysis of shotcrete on rock exposed to blasting. Licentiate thesis. Stockholm: KTH Royal Institute of Technology; 2012.
- Ahmed L. Laboratory simulation of blasting induced bond failure between rock and shotcrete. Stockholm: Rock Engineering Research Foundation. BeFo report 116, 2012.
- Ahmed L, Ansell A. Behaviour of sprayed concrete on hard rock exposed to vibration from blasting operations. Proceeding of 7th International Conference on Sprayed Concrete. Sandefjord: The Norwegian Society of Graduate Technical and Scientific Professionals, Tekna; 2014.
- Ahmed L, Ansell A. Experimental and numerical investigation of stress wave propagation in shotcrete. In: XXI Symposium on Nordic Concrete Research and Development. Hämeenlinna: Nordic Concrete Research; 2011.
- Ahmed L, Ansell A. A comparison of models for shotcrete in dynamically loaded rock tunnels. Proceedings of the 3rd international conference on engineering developments in shotcrete. Queenstown: Australian Shotcrete Society and the American Shotcrete Association; 2010.

Chapter 2

Impact-type vibrations

In this chapter a summary of relevant load types that cause impact-type vibrations is given. First, the characteristics of dynamic loads are commented. Then follows a discussion of important classes of loads that are mild or severe types of impacts, but also of traffic loads that are usually of nonimpact-types. However, the latter is included to provide background and motive for focusing on short duration vibration loads of high magnitudes, i.e. impact-type vibrations.

2.1 Dynamic load types

Vibrations acting on structures and constructions can have a variety of different external sources, including industrial, construction and transportation activities. An important first step in the dynamic analysis of a structure is to identify and characterize the dynamic loads that may occur. For concrete structures, this is important already from the time of casting. According to [20], a vibration may be classified as continuous with magnitudes that vary or remain constant with time, impulsive such as impact and shocks or intermittent, with the magnitude of each event being either constant or varying with time. All types of high magnitude vibrations may cause damage to young concrete but in most practical cases continuous vibrations are often of low magnitudes. Such vibrations, for example from machinery, steady road traffic, construction activities with e.g. tunnel boring machines, have therefore not been covered in this study. However, traffic vibrations will be commented in the following since several studies are published and the results are often referred to when vibration limits are discussed.

Examples of typical impulsive and intermittent vibration loads, expressed as function of strain rate, are given in [14] and here shown in Figure 2.1. Strain rate is the rate of change in strain of a material with respect to time and for e.g. an axially compressed bar it can be calculated as the speed at which the ends approach each other divided by the original length of the bar. From the figure, it can be seen that the highest strain rates occur from blasting that can generate strain rates within the range of $100 - 1000 \text{ s}^{-1}$. It should be noted that traffic vibrations, and also collisions, are associated with relatively low dynamic load levels. The higher load classes correspond to direct explosions, missile impacts, etc. Also, the material strength of concrete increases with strain rate and a dynamic increase factor (DIF), the ratio of the dynamic to the static value is, often used for this representation. The elastic modulus is also strain rate dependent, which is usually assumed to be due to a decrease in internal micro cracking for

increasing strain rates. As seen in the compilations of test results presented in Figures 2.2 – 2.3 there is little effect on the DIF at low strain rates, for both compressive and tensile loading. As a comparison it should be noted that in the CEB-FIP Model Code [33] a static compressive load is defined as corresponding to a strain rate of $3 \times 10^{-5} \text{ s}^{-1}$. However, from strain rates above approximately 1 s^{-1} there is a sudden increase in DIF, which is more obvious for the tensile strength. See e.g. [41, 42 and 47] for a thorough discussion of the subject, where also all the references given in Figures 2.2 – 2.3 are listed and commented. The load cases studied within this project generate strain rates that reach 1 s^{-1} . It should be noted that for blast loads the strain rate depends on the distance between the centre of the explosion and the point of observation, with increasing rates for decreasing distance. The strain rate levels in Figure 2.1 refer to close proximity blasting while blasting in situ during construction work usually generates strain rates in the same range as pile driving, i.e. around 1 s^{-1} [52]. It should also be noted that there are few investigations of the strain rate dependence of very young and hardening concrete. For the numerical examples presented in the following it is therefore assumed that any possible increase in material strength and elastic modulus due to strain rate effects is already accounted for and included in the material parameters used.

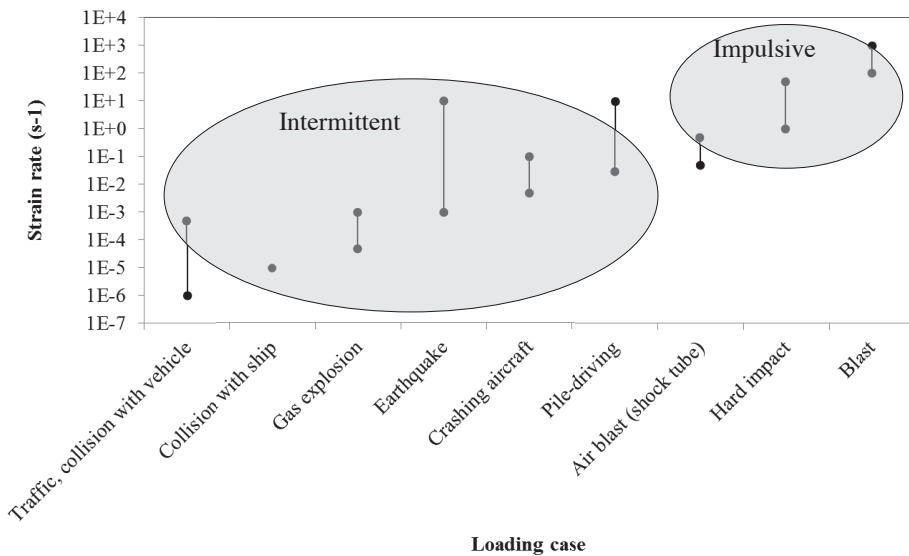


Figure 2.1: Approximate strain rate associated with various cases of loading, from [14].

Ungefärlig töjningshastighet i samband med olika fall av belastning, från [14].

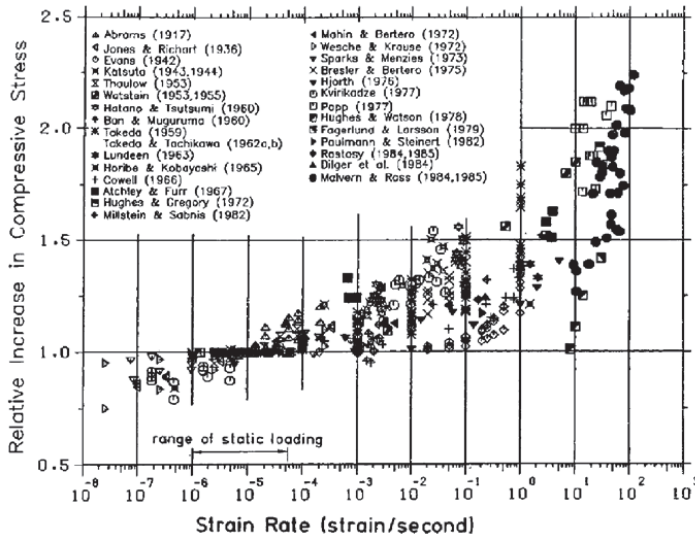


Figure 2.2: Strain rate effects on the concrete compressive strength, from [23].
Töjningshastigheters effekter på betongtryckhållfasthet, från [23].

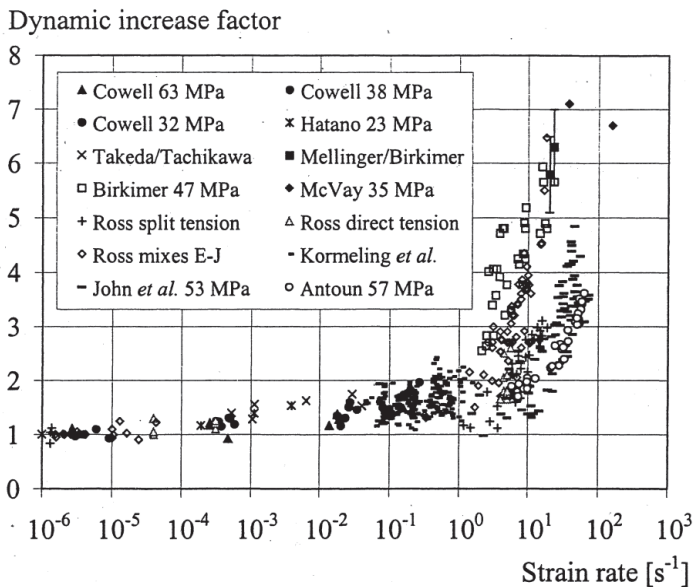


Figure 2.3: Strain rate effects on the concrete tensile strength. Reproduced from [42], based on [43]. *Töjningshastigheters effekter på betongdraghållfasthet. Hämtad från [42], där baserad på [43].*

The frequency content of dynamic loads is also an important parameter so an alternative classification of dynamic load on concrete structures is based on to the frequency contents and the amplitude, as seen in Figure 2.4. Generally, it can be seen that blast loading is associated with high frequencies and amplitudes, i.e. PPV, whereas both traffic and pile driving vibrations are associated with low frequencies but with high and low amplitudes, respectively. A comparison with the recommended maximum vibration velocities for young and hardening concrete is given in [11] and here later in Chapter 3. This gives values up to 180 mm/s, which is much lower than the range of 500-2000 mm/s representative for blasting in Figure 2.4. However, it should be noted that shotcrete damage has been documented to occur at 500-1000 mm/s, see [8 and 17], and that undamaged cast concrete subjected to 1800 mm/s of vibrations has been observed, see [40]. The frequency ranges given in Figure 2.4 should be seen as typical average values that may show large variation depending on ground type or structural stiffness. It should be noted that the compilation in [11] gives the frequency range for e.g. traffic vibration and pile driving as 1-100 Hz and for ground-borne blasting vibrations as 1-300 Hz. From the in situ measurements with shotcrete on hard rock [17] frequencies within the range of 150-2400 Hz were recorded.

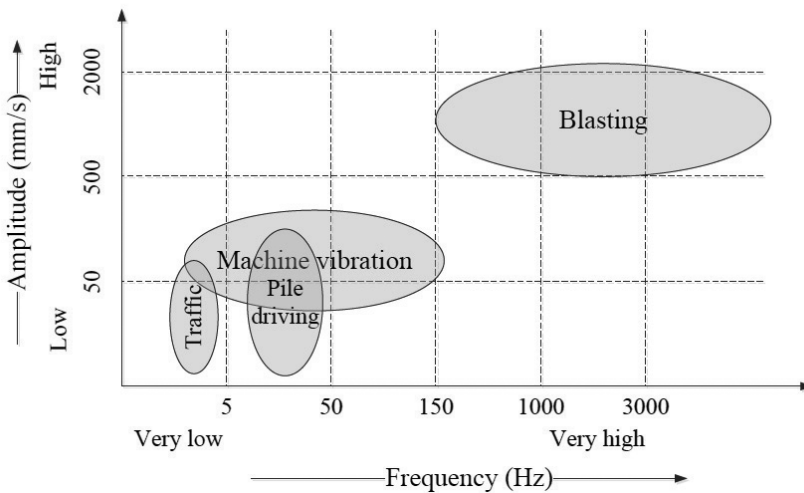


Figure 2.4: Frequencies and amplitudes for different dynamic loads, according to [29]. Figure is not to scale.

Frekvenser och amplituder för olika dynamiska belastningar, enligt [29]. Figuren är inte skalenlig.

2.2 Traffic vibrations

Traffic may generate vibrations that can be hazardous for the strength development of young and hardening concrete, and reduce the final bond of new concrete to existing concrete and reinforcement. The greatest concern is when repairs and rebuilding, e.g., bridge deck widening, is carried out while traffic is allowed to pass close to the construction site in adjacent lanes. Several researchers see, e.g. [31, 34 and 44], have found that vibrations caused by normal bridge

traffic have no detrimental effect on the concrete. None of these researchers identified any damage from traffic vibration, but nevertheless there are often concerns about permitting traffic on bridge decks during concrete-placing operations. An effective way to reduce the amplitude of traffic-induced vibrations is to maintain a smooth bridge deck surface and to avoid sharp approaches that could lead to impacts from heavy vehicles, [12]. In guidelines and technical specifications a maximum allowed traffic velocity is often given, e.g. in Norway 40 km/h has been set as a limit while Swedish guidelines restrict the velocity of heavier vehicles to 15 km/h, see [11 and 15]. The latter also restricted the vibration velocities to a maximum of 30 mm/s, [24], which could be compared with the much higher maximum vibration levels indicated in Figure 2.4. Thus, although the vibration levels generated may be high in some cases the restrictions assigned make traffic-induced vibration harmless to hardening concrete. However, a reduction in the bond to the reinforcing steel may occur in cases with large relative displacements between new and old concrete sections, which should be investigated through structural dynamic analyses. If old and early age concrete sections with its formwork are in synchronous movement the entire structure vibrates as a rigid body, and there will be little risk for damage due to traffic-induced vibrations. Therefore, as commented in [11], due to the low level of PPV, the relatively long duration of vibration and the need for structural dynamic analysis, traffic vibrations are not classified here as impact vibrations and therefore not accounted for in the numerical analyses.

2.3 Machine vibrations and pile-driving

Operating machines and impacts from pile driving generate vibrations with PPV similar to those of traffic but with slightly higher frequencies, as shown in Figure 2.4. There are few investigations of the effects from vibrating machines but some are referred to in [11]. Machines that generate heavy vibrations can be movable machines such as vibratory roller compactors but also static equipment, e.g. ball mills, crushers, pulverizers, compressors, forge presses, see also [32]. It has been observed that construction operating equipment and heavy operating machinery at building sites usually produce vibration velocities below 50 mm/s, which is in the lower range of what is indicated in Figure 2.4. An interesting study is presented by Krell [37]. Tests were done at a coal mill with equipment for pulverization of coal at a power plant. The machinery generated PPV levels up to 80 mm/s within the frequency range 0-200 Hz. The vibrations of the concrete foundation of the mill were recorded and maximum amplitudes were found for the frequency 46 Hz, which is in good agreement with the interval for machine vibrations in Figure 2.4.

Pile driving causes impact-type vibrations that propagate through the ground. However, the distance to newly cast concrete must be relatively short for damage to occur. As an example [56], with normal ground conditions and at a distance of 3 m standard pile driving will not often exceed 50 mm/s. This will only be critical for recently cast very young concrete, e.g. in foundations and slabs in direct proximity to the piling operations. However, strict vibration criteria are often used to obtain a safety factor for the operations and e.g. Siwula et al. [56] recommend that the pile driving activities within a radius of 3 m should not be carried out during the first 5 days after casting of normal concrete and earliest after 1 day for high early strength concrete. Low vibration levels are also reported by Bastian [22], who observed PPV levels around 10 mm/s around concrete close to piling operations. Further in situ tests with

young concrete close to pile driving are summarized by Akins and Dixon [10] and Dowding [27].

2.4 Blasting

Construction blasting in hard ground or rock results in stress waves that propagate outwards from the detonation centre, as stress waves that transports energy through the material. During their passage the particles within the material translates and returns to equilibrium, a motion that can be described as displacements, velocities or accelerations. When a wave front reflects at a free surface the particle velocities are doubled and a compressive wave reflects backwards as a tensile wave, etc. The velocity of propagation through elastic materials depends on the type of wave, the most important being longitudinal waves (P-waves) shear waves (S-waves) and Rayleigh waves, see e.g. Dowding [27]. The latter is a surface wave that carries the energy from a blast, or an impact, over long distances while P- and S- waves are more important at close range. Many researchers report blast damage criteria for hard rock and fully hardened concrete, for which the damage levels are often assumed to be close to identical. For Swedish hard rock, Persson [50] reported a PPV of 1000 mm/s as the limit for possible damage, for which Dowding [27] also reported cracking observed in a lined tunnel.

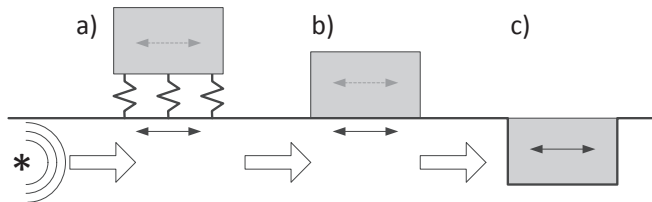


Figure 2.5: Effect from ground impact loads on structural concrete (a), aboveground concrete (b) and underground concrete (c), from [11].

Effekt av stötbelastningar i marken på konstruktionsbetong (a), betong ovan mark (b) och under marksbetong (c), från [11].

It has been shown that young concrete can withstand fairly high intensity impact vibrations during the first few hours after casting, see e.g. the reviews in [11-12]. However, the effect of frequency content is important but only addressed by a limited number of researchers, see e.g. [27, 39, 53 and 56]. Of the published safe vibration levels for young concrete close to vibrations that exist, the recommendations by Oriard and Coulson [49] are amongst the very few that also give the dependence of frequency. This is done indirectly by recommending a reduction factor that reduces the limit values when distance from the blast is increased, see [11]. This accounts for the fact that the frequency of motion lessens with distance, which results in increased particle displacement. This attenuation is caused by geometrical spreading and damping in rock or hard ground, [27]. When studying the effect of high intensity impact vibrations such as underground blasting, the type of concrete construction must also be considered. A classification into structural concrete, aboveground concrete and underground concrete, as

shown in Figure 2.5, is suggested in [11]. The major difference is here that un-restrained, aboveground structures are free to vibrate and respond as during an earthquake, while restrained, underground structures are forced to deform with the surrounding soil. In the latter case, propagating stress waves from e.g. an underground blasting will directly reach the concrete volume.

Chapter 3

Finite element analysis

The FE method is a powerful tool for study of structures subjected to dynamic forces. In this chapter, two-dimensional (plane strain) dynamic FE models of shotcrete and rock subjected to stress waves are presented, with the models, load formulations and boundary conditions described. The FE models are used to simulate the stress waves from blasting, propagating in rock towards shotcrete on a tunnel wall. Due to the inhomogeneous nature of the rock, the stress waves attenuate on its way from the point of explosion towards the shotcrete on the rock surface. This effect of material damping and the elastic modulus on the propagation of the stress waves are presented in [2].

3.1 Finite element models

Dynamic finite element models of rock and shotcrete subjected to stress waves have been developed using the Abaqus/Explicit finite element program [2]. The simulations were performed using two-dimensional (2D) plane strain elements. The models describe two cases with respect to the geometry of the tunnel and position of the detonation point. The fundamentals of the models are shown in Figure 1.1. An example of meshing and use of finite elements is shown in Figure 3.1, describing model of case (a) and case (b) in Figure 1.1. Note that only a short length of the tunnel is included for case (b). A fine mesh was used around the loading area and tunnel opening with coarser mesh further away from the tunnel opening. Infinite elements were utilized to represent the non-reflecting boundaries and prevent wave reflections. The rock and the shotcrete behave in a strictly elastic manner and possible failure thus occurs when the stresses at the shotcrete-rock interface exceeds the bond strength. That is, no plastic deformations or permanent failure, for example crushing or cracking, was considered in the models and a linear elastic relationship between stress and strain was assumed.

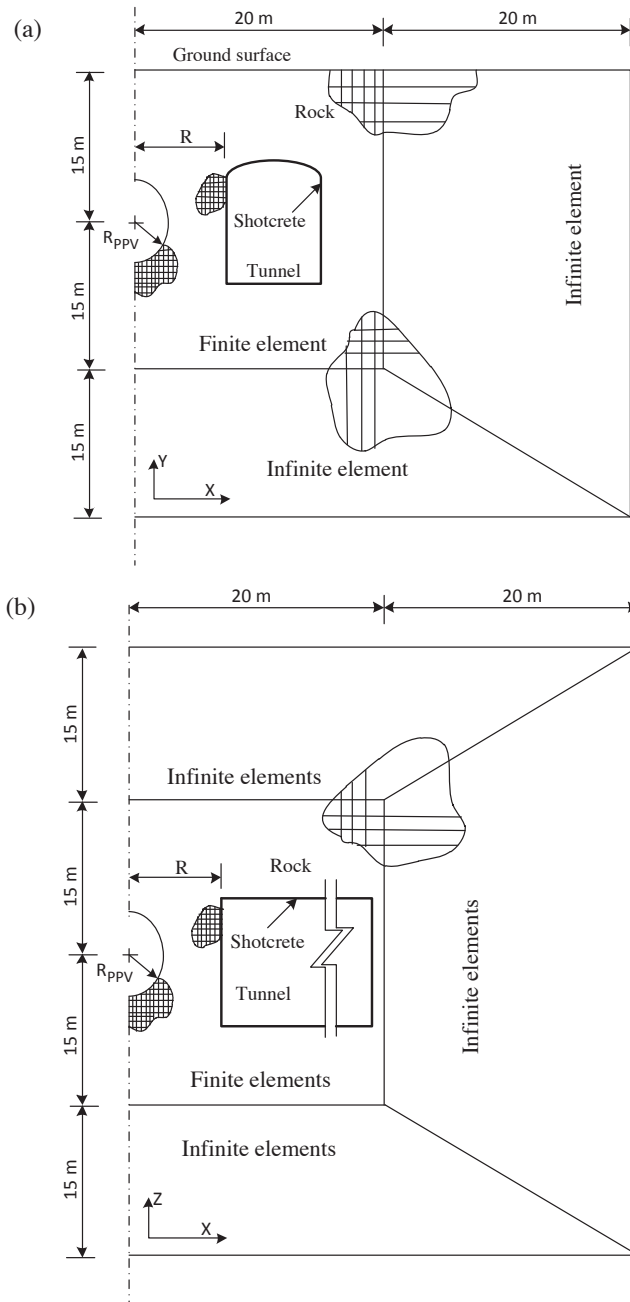


Figure 3.1: Configuration of finite element model; (a) tunnel profile (from [5]), and (b) tunnel plane (from [8]). *Konfiguration av den finita elementmodellen; (a) tunnelprofil (from [5]), och (b) tunnelplan (från [8]).*

The tunnel in case (a) is situated 11.5 m below the ground surface. The material surrounding the excavation is discretized with first-order 4-node plane strain elements of type “CPE4R”, recommended for simulations of impact and blast loading using Abaqus/Explicit [55]. The infinite extent of the rock is represented by a 20 m wide mesh that extends from the surface to a depth of 45 m. Far-field conditions on the bottom and right-hand side boundaries are modelled using infinite elements of type “CINPE4”. The interaction between rock and shotcrete was modelled using tie constraints, i.e. no relative displacement between the materials was assumed. The element size of the shotcrete part is $0.01 \times 0.1 \text{ m}^2$ for all models, with different element sizes used for the rock part. Depending on the accuracy and details of the solution, some regions of the rock are discretized with a refined mesh. More refinement adjacent to the tunnel opening and loading area was made, due to the significant deformations expected at these regions. The model consists of about 28000 nodes and 2500 elements.

The detonation is introduced in the model from a circular area within the rock where an incident particle velocity is applied. An incident PPV wave caused by the explosion is applied as a boundary condition at the perimeter of the circular area, with the radius R_{PPV} chosen so that the included rock remains undamaged outside this area. For Swedish hard rock, a PPV damage criterion is given by Persson [50], where the threshold damage (incipient damage) occurs at 1000 mm/s. In the following examples a damage limit at 900 mm/s for granite is assumed, which is on the safe side with respect to incipient damage [50]. From Eq. (1.1), the depth of the damage zone R_{PPV} , where the particles velocity reaches the threshold PPV, will be given by

$$R_{ppv} = 0.846 \sqrt{Q} \quad (\text{m}) \quad (3.1)$$

where R_{ppv} is the depth of the damage zone into the rock mass measured from centre of the charge to where the particles velocity reaches the threshold PPV. This distance thus corresponds to the limit for rock damage and therefore elastic properties can be assigned to the rock outside this area. In the real case, the rock area immediately around the hole containing the explosives will be severely cracked. However, there is no need to include this effect in the present model since the load here is applied at a long enough distance from this point. To allow the stress wave to disperse a relatively large volume of rock is modelled, compared to the distance to the centre of the explosives. The integration method used for calculating the response is exact for loads that vary piecewise linearly with time. Therefore, it is better to define the load-function of each node at the charge hole as tabular data. To reduce the effect of the numerical differentiation, a smooth curve of velocity time history is used with $\Delta t = 0.01 \text{ ms}$. To define the velocity at each node n , global Cartesian coordinate components are used as shown in Figure 3.2. The two components depend on the angle γ of the resultant velocity to the x -axis. Each component describes the velocity components in the given direction at one node.

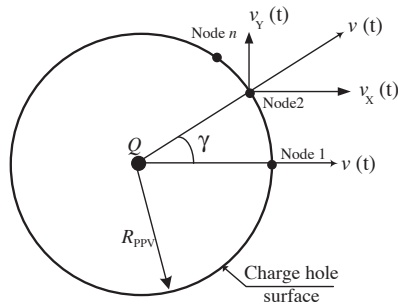


Figure 3.2: Components of the incident velocity at each node.

Komponenter hos den infallande hastigheten vid varje nod.

By applying a particle velocity at the charge hole as a velocity boundary condition, the propagation of the waves in the rock was investigated. In the examples presented in [2], a damping ratio of 8% is used, estimated from in situ measurements. The shotcrete was assumed to have a density of 2100 kg/m^3 , a modulus of elasticity of 27 GPa. The rock, a density of 2500 kg/m^3 and a modulus of elasticity of 40 and 16 GPa for intact and fractured rock, respectively. The detonation of $Q = 2 \text{ kg}$ of explosives, corresponding to ANFO (ammonium nitrate and fuel oil), is considered for series of calculations for the two cases in [2]. The principal frequency of the incident particle velocity is assumed to be 2000 Hz for all models. Results for 100 mm thick shotcrete are calculated. Also, examples demonstrating the effect of shotcrete age are presented, for detonation of Q equal to 0.5, 1.0 and 2.0 kg, respectively. The dynamic excitation can be described as a cosine-pulse velocity or a corresponding sine-pulse acceleration [8].

3.2 In-situ case

A dynamic finite element model of rock and shotcrete that represent case (b) in Figure 1.1 has been developed by including the effect of both intact rock and a zone of rock fractured due to blasting. This was due to the inclusion of a 0.5 m section of fractured rock that contributed to the reflection, transmission and superposition of stress waves. The modelling results have been verified through comparison with in situ observations and measurements.

The results from the in situ investigation presented in Section 1.4, by Reidarman and Nyberg [51] at the Southern Link (Södra länken), are well suited for evaluation of the finite element models described in the previous section. No shotcrete damage was observed following the blasting, due to the very strict guidelines used, and it can thus be assumed that the shotcrete-rock system behaves elastically throughout the passage of the stress waves. The FE model, based on elastic material properties, can therefore be used for a numerical study of the stress wave propagation along these tunnel walls. For this case study, a 2D model of the horizontal tunnel plane is used (see Figure 1.1(b)), since a full 3D model would have been much more computationally demanding. The model describes the same deformations as the measurement set up used in [51], with accelerometers positioned on a horizontal line along the tunnel length. The model describes the wave that propagates through the rock from the detonation point at the centre of the charge towards the front of the tunnel and along the tunnel sides. An example of meshing and use of finite elements are shown in Figure 3.3. The detonation is introduced in the

model from a circular area within the rock where an impulsive particle velocity is applied. The incident PPV wave caused by an explosion is applied as previously described in Section 3.1, i.e. as a boundary condition at the perimeter of the circular area with the radius R_{ppv} . The model consists of about 27000 nodes and 26000 elements and the analysis example is based on the material properties given in [6], valid for cases with 100 mm thick shotcrete.

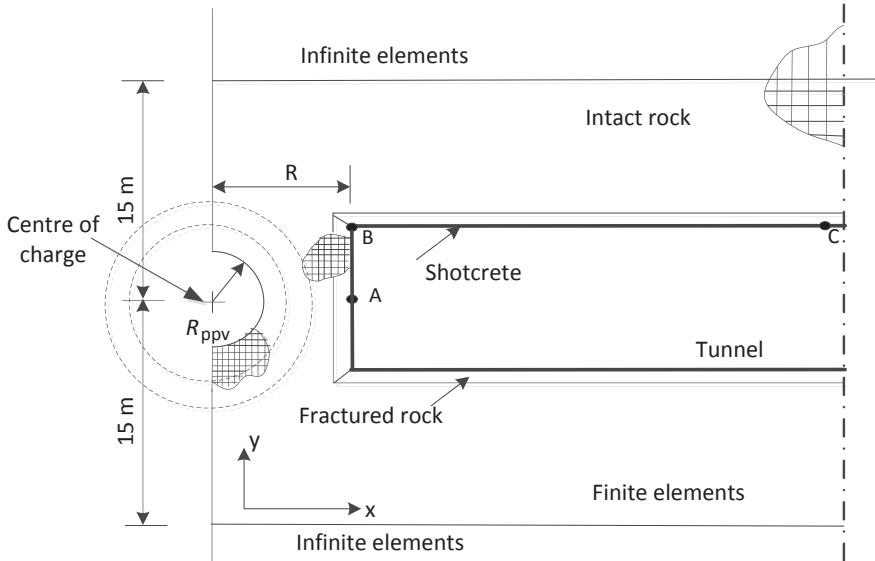


Figure 3.3: Detonation in rock ahead of the tunnel face (horizontal plane) in the Southern Link. Configuration of finite element model [6].

Detonation i berget framför tunnelfronten (horisontalplanet) i Södra Länken
Konfiguration av finit elementmodell [6].

Chapter 4

Numerical results

Numerical results from different models are presented in this chapter. The propagation of the waves in the rock was investigated by applying a particle velocity at the charge hole as a velocity boundary condition. The FE models consist of rock and infinite boundary conditions without the tunnel opening. The rock is assumed to be intact or fractured with the modulus of elasticity equal to 40 and 16 GPa, respectively. In the first examples, the two cases described in Section 3.1 are studied using different amounts of explosives, followed by an example based on the in-situ case described in Section 3.2.

4.1 Tunnel profile and plane

Results from a series of models with varying distance between shotcrete and explosive charges are presented in [8]. Results for the two cases of the horseshoe shaped tunnel profile and the tunnel plane in Figure 1.1 is here included (Figures 4.1 – 4.4) to show how the explosion generates stress waves that propagate towards the shotcreted tunnel walls. Due to this motion, the stresses in the shotcrete vary with time, being the sum of the incident and reflected stress waves. The calculations were carried out with $R = 3.0$ m from the centre of the charge. The same boundary conditions as used in [2] are assumed. The stresses in the x- and y-directions are presented in Figures 4.1–4.4 and indicated with red areas are tensile stresses (positive) over 0.2 MPa and with blue compressive stresses (negative) lower than -0.2 MPa. Far away from the charge hole and the tunnel, zero stress (green) can be assumed.

A feature of finite element stress analysis is the large amount of data generated, making the information suitable for presentation in graphical form. The stress distributions due to blasting loads applied as boundary conditions at the perimeter of the circular area with the radius R_{PPV} , are shown in Figures 4.1–4.4. The stresses that are developed around horseshoe shaped tunnel profiles are depicted. Shortly after the explosion, the compressive stress waves in the x-direction (σ_x) reach the tunnel and are transmitted into the thin layer of shotcrete on the rock surface. Then, the compressive stress waves start to reflect at the surrounding rock, as shown in Figure 4.1. Reflected, tensile stress waves appear on the upper and lower sides of the shotcrete layer, continuing towards the end of each side and being concentrated around the corners. In Figure 4.2, the contour of the stresses in the y-direction (σ_y) are depicted. It can be seen that the reflected tensile stresses appear only on lower sides of the tunnel. It should be pointed out that the time span of the analyses are 10 ms and absorbing boundaries were used to

eliminate stress wave reflection from the outer edges of the models, beyond which the rock continues.

The models of Figures 4.3–4.4 demonstrate detonation ahead of a tunnel front and the stresses that are developed along the tunnel walls, see [8]. The centre of the explosive charge was here located 3 m from the front. Compared with the results in [2], this is a safe distance with respect to damage at the front where the vibration velocity is $v_{\max} = 470$ mm/s, as given in [8], i.e. just below the previously defined damage limit of 500 mm/s, [17]. The results in Figure 4.3 show dominance by stresses along the tunnel walls; i.e. in the z-direction (σ_z). Of the three previously used engineering models in [5], shear stresses could only be described by the beam-spring model. In the study of large scale blasting during mining operations [16] where stress waves reach the shotcrete at an oblique angle, domination of shear stresses was also observed. It can be seen that the only high normal stresses (x-direction) appear locally just behind the tunnel face while the maximum shear stresses (z-direction) are situated 2 m into the tunnel. In addition, the shear stresses are present more than 10 m into the tunnel. See [2], for more details. Figure 4.4 shows that after the explosion the tensile stresses in the x - direction (σ_x) appeared on both shotcreted sides of the tunnel.

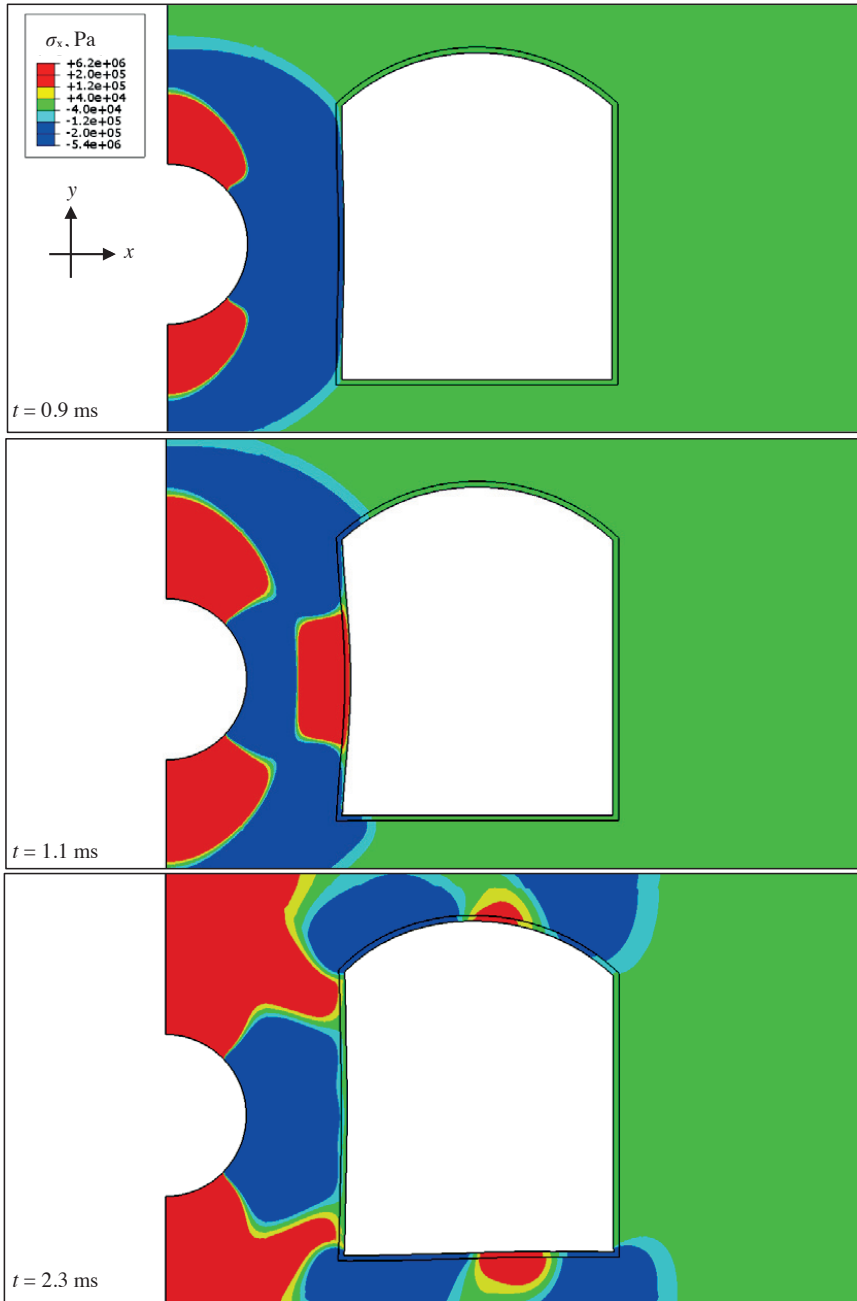


Figure 4.1: Contours of stresses in x-direction (σ_x) of horseshoe shaped tunnel. Deformation scale 1:1000, from [8].

Konturer av spänningar i x-riktningen (σ_x) i en hästskeformad tunnel. Deformationsskala 1: 1000, från [8].

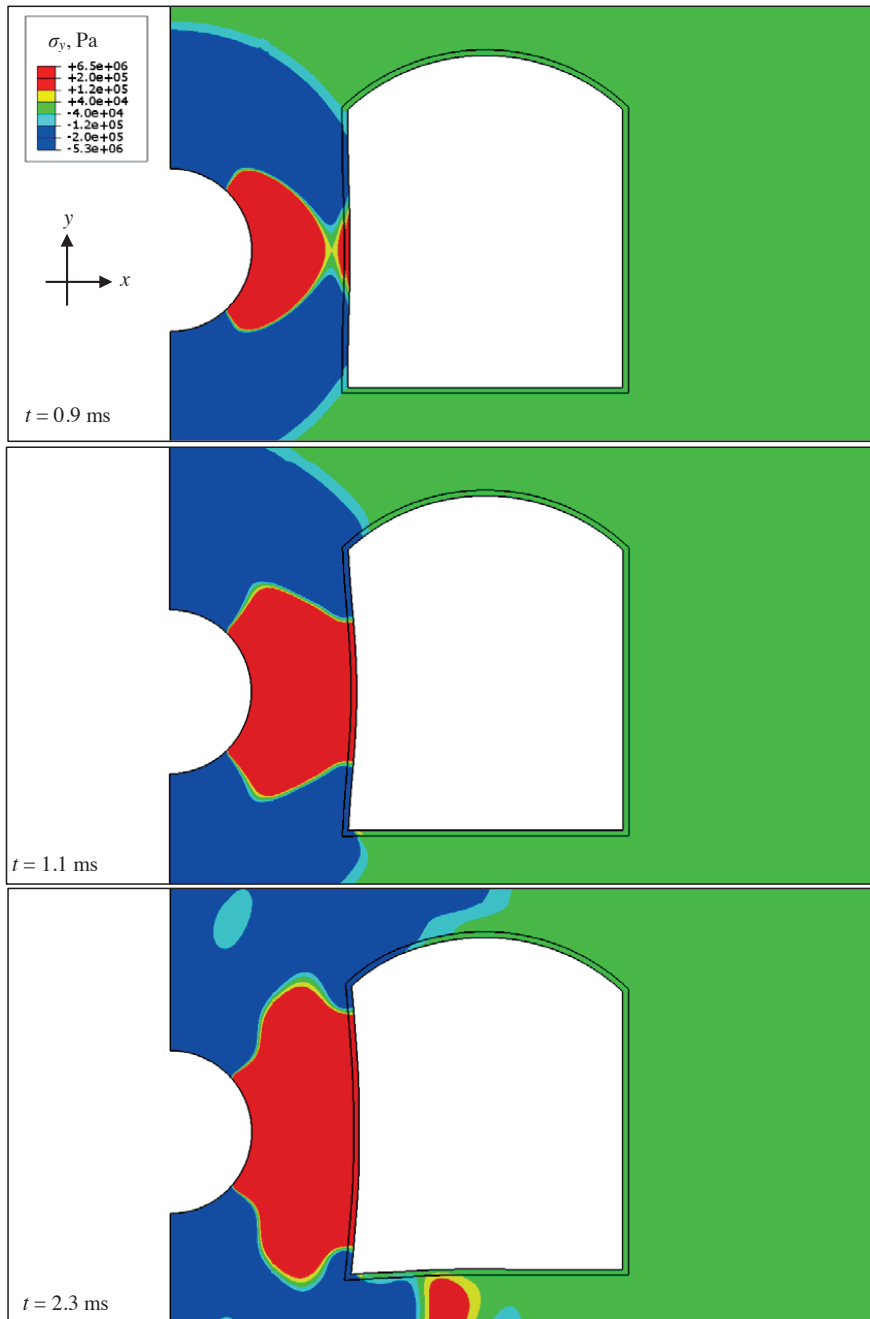


Figure 4.2: Contours of stresses in y-direction (σ_y) of horseshoe shaped tunnel. Deformation scale 1:1000, from [8]. *Konturer av spänningar i y-riktningen (σ_y) i en hästskeformad tunnel. Deformationsskala 1: 1000, från [8].*

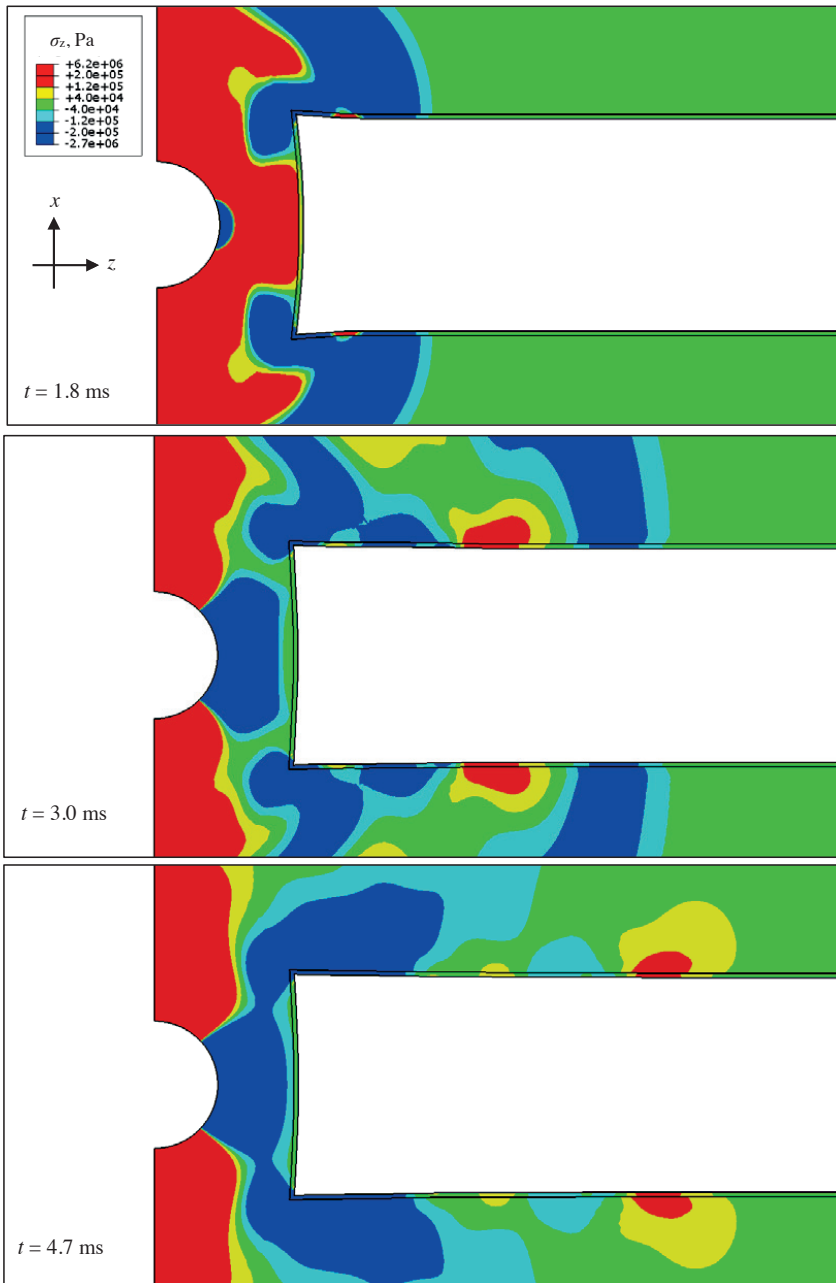


Figure 4.3: Contours of stresses in z -direction (σ_z) of the side walls of the tunnel. Deformation scale 1:1000, from [8]. *Konturer av spänningar i z -riktningen (σ_z) i sidväggarna i tunneln. Deformationsskala 1: 1000, från [8].*

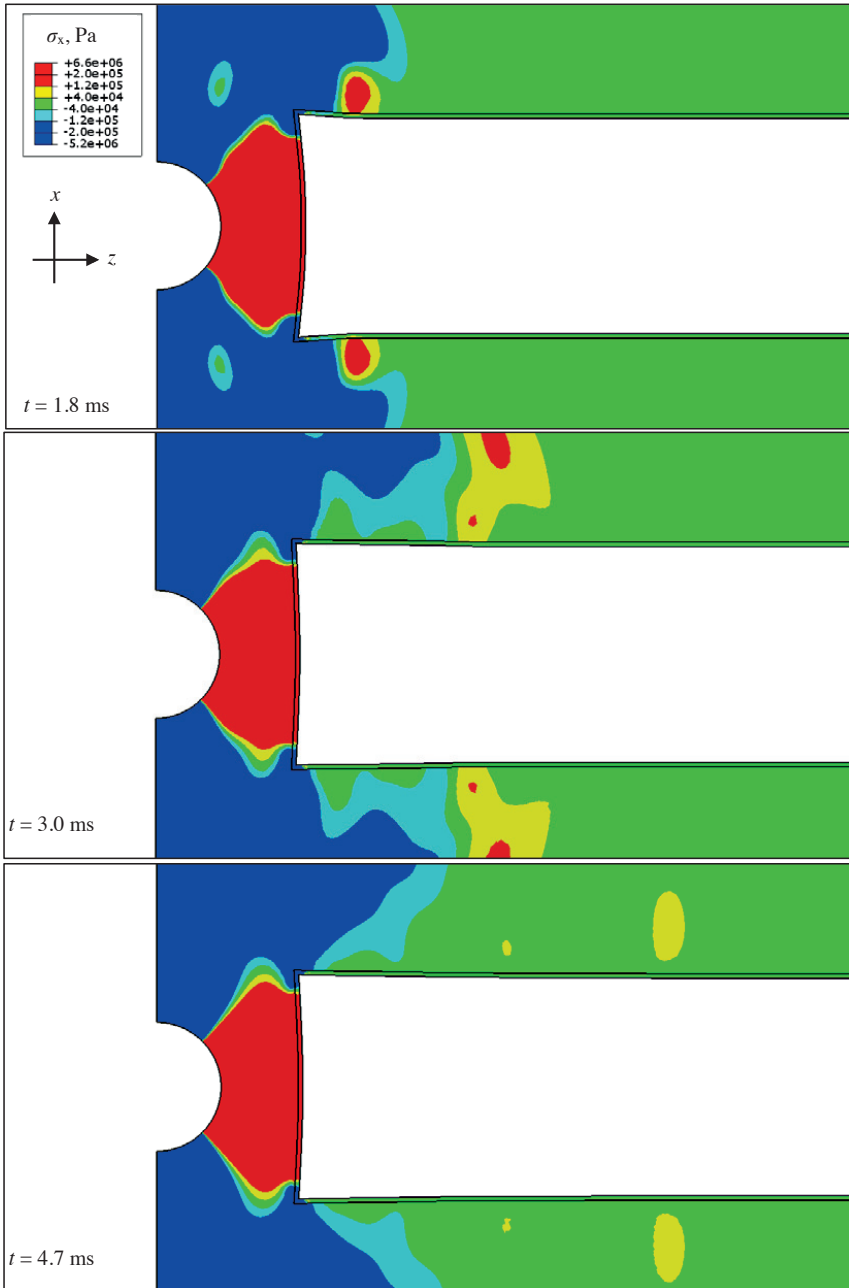


Figure 4.4: Contours of stresses in x -direction (σ_x) of the side walls of the tunnel. Deformation scale 1:1000, from [8]. *Konturer av spänningar i x -riktningen (σ_x) i tunnelns sidoväggar i tunneln. Deformationskala 1: 1000, från [8].*

4.2 In-situ case

The response of the shotcrete in the tunnel is investigated for various blast loads, using 2 and 3 kg of explosives in [6]. Under the higher blast loads, the shotcrete stress along the tunnel length increased, giving stress concentrations of which an example can be seen in Figures 4.5–4.6, where the stress distributions are shown. The stresses in the x- and y-directions are indicated with red areas showing tensile stresses (positive) over 1.0 MPa and blue showing compressive stresses (negative) lower than -1.0 MPa. Far away from the charge hole and the tunnel, zero stress (green) can be assumed. It can be seen that at 2 ms after the detonation, the first peak of shear stress, see Figure 4.5, is concentrated mainly at the tunnel front while at 2.7 m peaks of high shotcrete stress can be seen forming close to the corners between front and wall, see Figure 4.6. Such stress concentrations also propagate along the tunnel walls, but with decreasing stress levels. It should be pointed out that the analysis covered 100 ms duration.

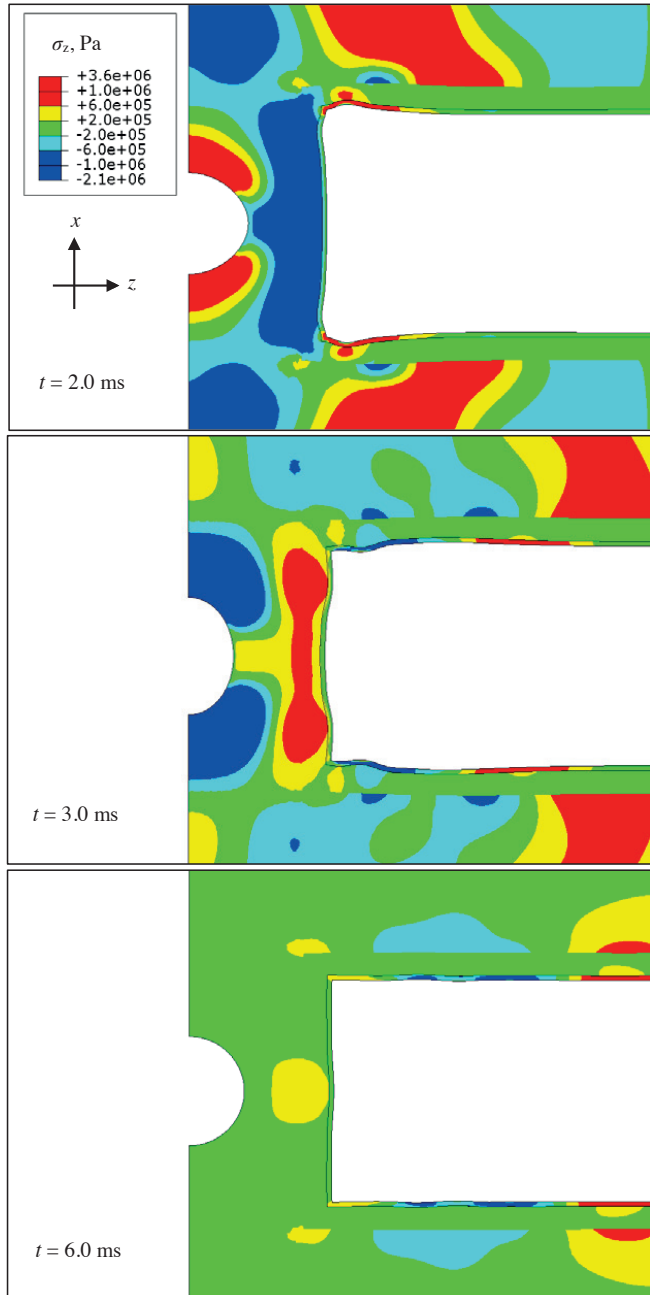


Figure 4.5: Contours of stresses in z-direction (σ_z) of the sidewalls of the tunnel. Deformation scale 1:1000. *Konturer av spänningar i z-riktningen (σ_z) i tunnelns sidoväggar. Deformationsskala 1: 1000.*

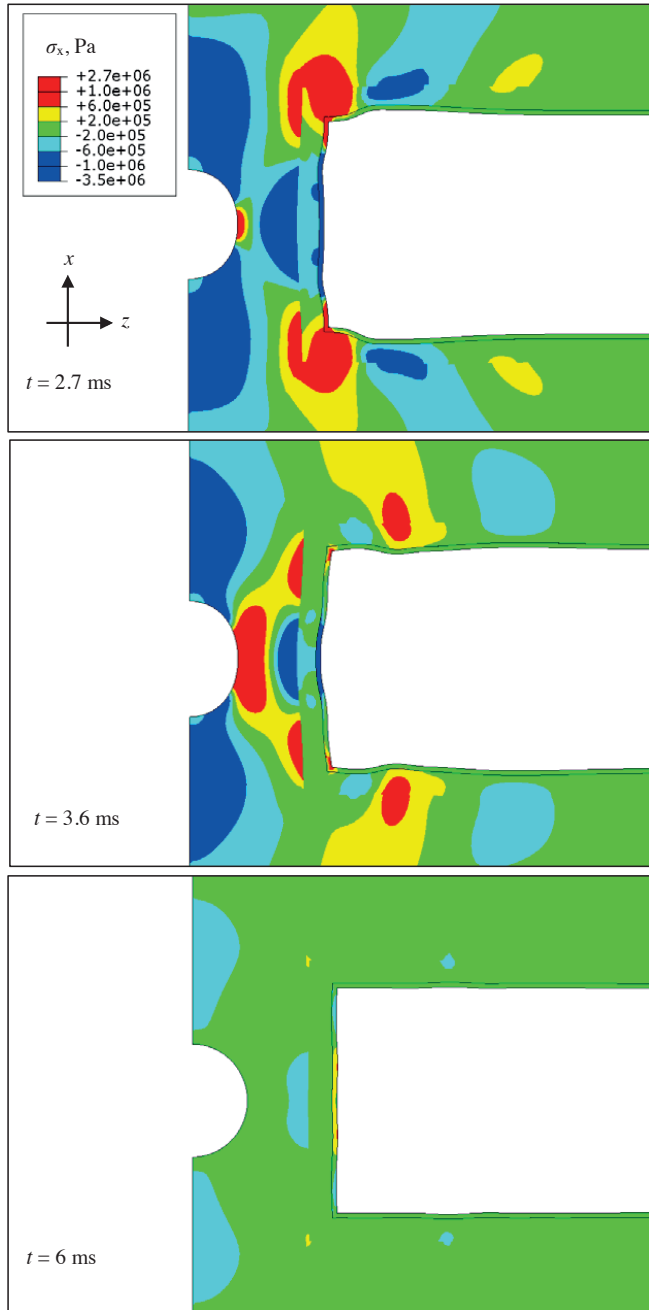


Figure 4.6: Contours of stresses in x-direction (σ_x) of the sidewalls of the tunnel. Deformation scale 1:1000. Konturer av spänningar i x-riktningen (σ_x) i tunnelns sidoväggar. Deformationsskala 1: 1000.

Chapter 5

Impact vibration limits and guidelines

Important vibration criteria and published guidelines are evaluated and assessed in [2-6 and 11] within this project. The most important of these are summarized here to provide guidance on what might be appropriate choices for practical use. Based on the state-of-the art report in [11], a summary of vibration criteria for young and hardening concrete and shotcrete subjected to vibration from impact-type loads and blasting is first given. These criteria are published by national standards institutes or organizations. Then, a section that comments on the recommendations and guidelines given in [3 and 6] follows, for young concrete subjected to impact-type loads. Recommendations for shotcrete, young and also fully hardened, are given in the last section. The latter are based on analytical modelling [5], laboratory testing [4] and finite element modelling [2 and 6], and also compared with previous results from [8].

5.1 Standards and specifications

Previous research objectives have included determination of threshold levels for human perception of vibrations, as well as preventing and assessing damage to structures and buildings. The effects of vibrations on young and curing concrete have been addressed by relatively few, and a large variation in research recommendations are found due to the absence of in-depth understanding of exactly how the vibration would cause damage to e.g. curing concrete. For curing concrete, vibration limits are prescribed in some codes, standards and specifications or as recommendations compiled by researchers and practicing engineers. A summary of such general national standards that include vibration close to young and hardening concrete is presented in Table 5.1. More detailed recommendations with respect to young concrete can be found in [11] where it is also concluded that recommendations in national standards and specifications often are conservative, giving values that often are 10 times below what can be observed in situ or in laboratory environments.

In tunnelling, the use of shotcrete is often restricted near the area where blasting takes place, due to the risk of damaging recently applied shotcrete. There are no limit levels for blasting-induced vibrations given in the standards but only recommendations on e.g. minimum compressive strength of concrete or shotcrete. For example, it has been prescribed that the compressive strength should be at least 6 MPa [58] or that the concrete must have reached a strength level of around 60% of the final compressive strength [30] in order to withstand nearby blasting. As a complement to the latter requirement, it is also recommended that the maximum

PPV must not exceed 10 mm/s for shotcrete up to 3 days old. For shotcrete 3–7 days old, the limit is 35 mm/s, and 110 mm/s for shotcrete older than 7 days.

Table 5.1: A comparison of some national standards and specifications for vibrations close to young and hardening concrete, from [11].

En jämförelse mellan några nationella standarder och specifikationer för vibrationer nära ung och hårdnande betong, från [11].

| Concrete age: | 0–3 days | 3–7 days | 7–28 days | >28 days | Comments: |
|---------------|------------|------------|--------------|----------|----------------------|
| USA | - | 6 mm/s | 51 mm/s | - | |
| China | 15–20 mm/s | 30–40 mm/s | 70–80 mm/s | - | ≤ 10 Hz |
| | 20–25 mm/s | 40–50 mm/s | 80–100 mm/s | - | 10–50 Hz |
| | 25–30 mm/s | 50–70 mm/s | 100–120 mm/s | - | ≥ 50 Hz |
| Norway | 5–50 mm/s | 50 mm/s | 70 mm/s | 100 mm/s | |
| Finland | 45 mm/s | 50 mm/s | 70 mm/s | 70 mm/s | Distance 1 m |
| | 90 mm/s | 100 mm/s | 140 mm/s | 140 mm/s | Distance 10 m |
| Sweden | - | - | - | 70 mm/s | Distance 1 m |
| | - | - | - | 134 mm/s | Distance 10 m |
| | 30 mm/s | 30 mm/s | - | - | If $f_c \leq 12$ MPa |

5.2 Young concrete vibration limits

The traditional opinion has been that blasting vibrations up to e.g. 50 mm/s is no threat to early age curing concrete. However, a considerable amount of research has been done to investigate how vibration effects from single events such as a dynamite blast close to young concrete affects its material properties and performance when fully hardened, see e.g. [40]. The published studies and observations have often been carried out under different conditions that make comparison difficult. However, based on the literature survey in [11] the recommended limits shown in Figure 5.1 are selected as representative for young concrete subjected to impact-type vibrations. For a time span of up to seven days, the recommended vibration criteria are given as maximum allowed PPV. On basis of Figure 5.1, recommended maximum vibration velocities are given in Table 5.2, valid for normal strength concrete, cured at +20°C and subjected to short duration impact-type vibrations at close range, also with recommended limits for corresponding continuous vibrations. Detailed recommendations based on finite element modelling are presented in Table 5.3, with respect to very young concrete, i.e. concrete younger than 12 hours. Recommended damage limits at concrete ages of 4, 6, 8 and 12 hours are given, based on calculations for concrete strength classes C25 and C50, as described in [3].

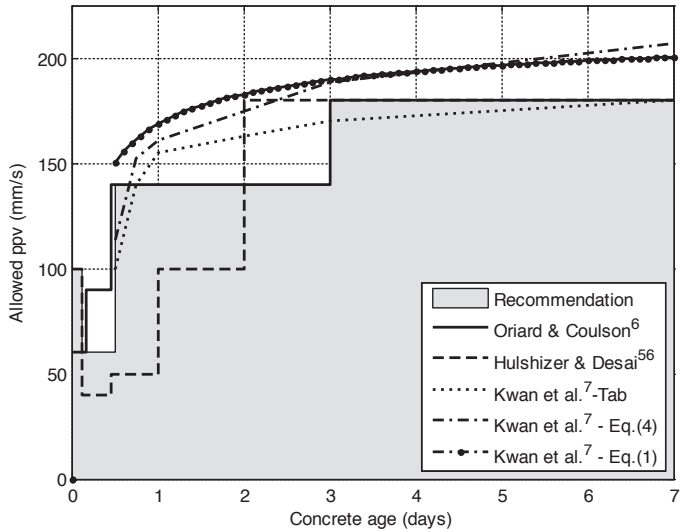


Figure 5.1: Comparison of recommended maximum PPV as function of age for young and hardening concrete. The recommended values from Table 5.2 are shown as a shaded area according to [11].

Jämförelse av rekommenderade maximala PPV som funktion av ålder för ung och hårdnande betong. De rekommenderade värdena från Tabell 5.2 markeras med en skuggad yta, enligt [11].

Table 5.2: Recommended PPV for young concrete in mm/s, from [11]. The limits for continuous vibrations are according to [31].

Rekommenderas PPV för ung betong i mm/s, från [11]. Gränserna för kontinuerliga vibrationer enligt [31].

| Vibration type | Concrete age | | | | | |
|----------------|--------------|------------|----------------|----------|----------|----------|
| | 0–3 hours | 3–12 hours | 12 hours–1 day | 1–2 days | 2–3 days | 3–7 days |
| Impact | 100 | 60 | 140 | 140 | 140 | 180 |
| Continuous | (100) | 40 | 40 | 100 | (140) | (180) |

Table 5.3: Recommended PPV damage limits for early age concrete, from finite element calculations presented in [3].

Rekommenderade PPV skadegränser för ung betong, från finita elementberäkningar presenterade i [3].

| Concrete age, hours | Concrete class C25 | | Concrete class C50 | |
|---------------------|------------------------|------------------------|------------------------|------------------------|
| | PPV lower limits, mm/s | PPV upper limits, mm/s | PPV lower limits, mm/s | PPV upper limits, mm/s |
| 4 | < 30 | † | 30 | † |
| 6 | 40 | † | 50 | 90 |
| 8 | 50 | 80 | 70 | 100 |
| 12 | 60 | 110 | 100 | 200 |

† Not possible to obtain upper limits

5.3 Shotcrete vibration limits

The performance of young and hardened shotcrete exposed to high magnitudes of vibration is investigated in [2, 4-6]. Safe distances and shotcrete ages for underground and tunnelling construction is discussed, using numerical analyses and comparison with measurements and observations summarized in [8 and 13]. Examples of preliminary recommendations for practical use are given in [8] and it is demonstrated how the developed models and suggested analytical techniques can be used to obtain further detailed limit values.

For fully hardened shotcrete, the three analytical models presented in [5] are used for calculations of examples for three different shotcrete thicknesses; 100, 50 and 25 mm. The recommendations for minimum safe distances to a point of detonation of $Q = 2$ kg of explosives are given in Table 5.4. The results are calculated for two different incoming stress waves with $f = 2000$ Hz and $f = 1265$ Hz and with propagation velocities through the rock equal to $c = 4000$ m/s and $c = 2530$ m/s, corresponding to $E = 40$ GPa and $E = 16$ GPa for the rock, giving the results shown in Figure 5.2. Table 5.4 thus gives a comparison between values for varying rock quality and load frequencies. To represent the occurrence of cracks and imperfections of rock a lower value of the modulus of elasticity is considered, thus the safe distances for $f = 1265$ Hz are lower than for $f = 2000$ Hz. The results from [18] are also given for comparison. Note that an increase in load frequency leads to higher load levels and longer safe distances.

The results presented in [2 and 6] are used as a basis for recommendation of minimum ages of shotcrete at the time of blasting, exemplified with the recommendations for 100 mm thick shotcrete that are compiled and presented in Table 5.5. Three different shotcrete types are included, with their development of bond and tensile strength shown in Figure 5.3. The results from [16] are given for comparison as representative for slow hardening shotcrete with waterglass (Sodium silicate) and low temperature curing. It is recommended [4] that the maximum allowable PPVs at the interface between shotcrete and rock are 250 and 500 mm/s within 0–1 day and >1 day, respectively. The results in Table 5.5 are calculated for detonations

of 0.5, 1.0, 2.0 and 3.0 kg of explosives at 2.2, 3.0 and 5.0 m from shotcrete on a granite rock surface. The results are obtained from comparison with the bond and tensile strengths given in Figure 5.3, see [6].

Table 5.4: Recommended minimum safe distance for fully hardened shotcrete and detonation of $Q = 2$ kg explosives, from [8].

Rekommenderade minsta säkerhetsavstånd för fullhård sprutbetong vid detonation av $Q = 2$ kg sprängämne, från [8].

| Rock and load characteristics | Shotcrete thickness | | |
|---------------------------------------------------|---------------------|-------|-------|
| | 100 mm | 50 mm | 25 mm |
| $E_{\text{rock}} = 16$ GPa and $f = 1265$ Hz | 1.8 m | 1.0 m | 0.7 m |
| $E_{\text{rock}} = 40$ GPa and $f = 2000$ Hz | 2.5 m | 1.5 m | 0.8 m |
| $E_{\text{rock}} = 40$ GPa and $f = 2500$ Hz [18] | 3.5 m | 1.9 m | 1.2 m |

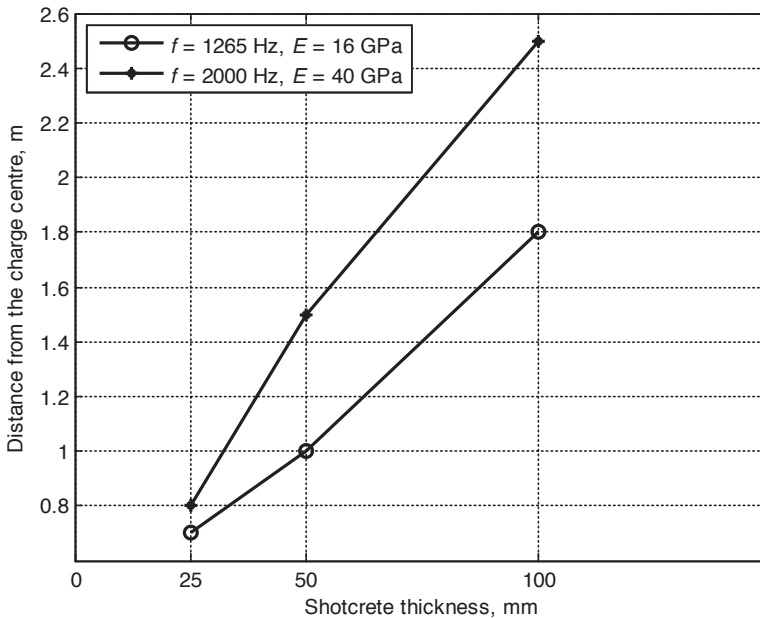


Figure 5.2: Compiled minimum safe distances from detonation of $Q = 2$ kg. Dependence of load frequency f and rock modulus of elasticity E , [8].

Sammanställda minsta säkerhetsavstånd från detonation av $Q = 2$ kg. Beroende av lastens frekvens f och betongs elasticitetsmodul E , [8].

Table 5.5: Recommended minimum ages in hours for 100 mm thick shotcrete of three types. The strength development is shown in Figure 5.3.

Rekommenderad minimiålder i timmar för 100 mm tjockt sprutbetong av tre typer. Hållfästets utvecklingen visas i Figur 5.3.

| | Distance form explosive | | | | | | | | | |
|----------------------|-------------------------|-------|-------|-------|-------|-------|-------|-------|-------|-------|
| | 2.2 m | | | 3.0 m | | | | 5.0 m | | |
| Explosives: | 0.5kg | 1.0kg | 2.0kg | 0.5kg | 1.0kg | 2.0kg | 3.0kg | 0.5kg | 1.0kg | 2.0kg |
| Ahmed [8] | 12 | 18 | * | 10 | 13 | 21 | - | 7 | 9 | 12 |
| Ansell [16] | >24 | >48 | * | 24 | >24 | >48 | - | 9 | 21 | >24 |
| Ahmed and Ansell [6] | - | - | - | - | 12 | 15 | 23 | - | - | - |

* Not possible to obtain a sufficiently high bond strength. - Data not calculated.

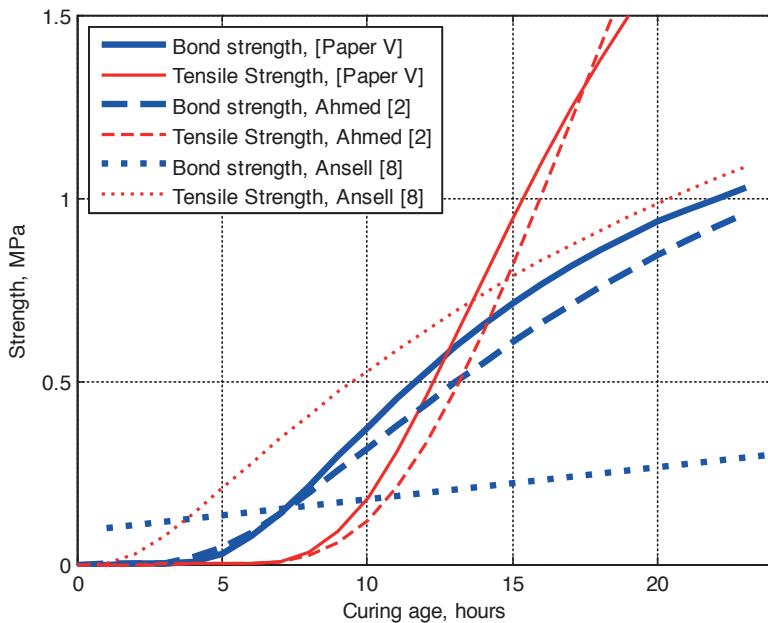


Figure 5.3: Bond and tensile strength vs curing age for the young and hardening shotcrete types referred to in Table 5.5.

Vidhäftnings- och draghållfasthet vs härdningsålder för de unga och hårdnande sprutbetongtyper som avses i Tabell 5.5.

Chapter 6

Recommendations and conclusions

The project has been interdisciplinary, combining structural dynamics, finite element modelling, concrete material technology, construction technology and rock support technology. After an initial project phase with focus on vibration and young shotcrete on hard rock the perspective has been widened also to include young, cast concrete, more details provided in [9]. This has been possible since the analytical methods and models used have been applicable and possible to develop for both cases. The general scope of the project is thus young concrete and impact-type vibrations but it also includes a comparison between cast and sprayed concrete. In the following, the main conclusions are given, regarding load types, testing techniques and differences between young cast and sprayed concrete.

6.1 Load type

A comparison between different dynamic loads that can act on young and hardening concrete shows that impact-type loads are by far the most serious, see [11]. None of the other possible load types result in equally high load levels, expressed as either vibration velocity, acceleration or strain rate, see Figure 2.1 and 2.4. This load type is also characterized by relatively high frequencies and short duration. Typical impact loads are direct mechanical impacts, vibrations from blasting and e.g. seismic vibrations from earthquakes and dynamic fallout of rock masses due to high rock stresses. Pile driving is also regarded as an impact load but the stress propagation here usually takes place in soils softer than rock, which combined with common practical distance to concrete structures often leads to relatively low levels of vibration. Traffic loads often represent another type of load and can be classified as intermittent and of relatively long duration. However, uneven road surfaces can lead to impact-type loads during passage of heavy vehicles but these usually correspond to moderate intensities of vibrations. Damage that occurs during repair of bridges with passing traffic is due to relative displacements between old and new concrete sections and should thus be analysed with structural dynamics or quasi-static methods. In the analysis of the vibration sensitivity for concrete structures, clear definition of the case studied should be made with the choice of analysis methods based on this. For young concrete structures affected by impact loads, it is here recommended that a classification into three types is made; structural concrete, concrete aboveground and belowground concrete. For the first type, the natural frequencies and dynamic properties of the structure are critical and therefore a specific structural dynamic analysis must be performed in these cases. Here, an example is a newly cast concrete slab supported by weak columns and possibly formwork

structures. The situation of more compact concrete structures on the ground is equal to the case of earthquake loads resulting in inertial forces and rigid body displacements. The case with shotcrete on rock subjected to blasting vibration can be described in this way. The perhaps most important of the three cases, is structures below ground where impact waves can propagate directly into the concrete volume, see Figure 2.5, possibly resulting at high levels of vibration. These concrete structures are also confined and follow the movement of the surrounding soil or rock without relative deformation. Besides being the case for which the maximum vibration levels may appear, it is also the case where defined vibration limits will be most relevant.

6.2 Test results and measurement

In the case of in situ testing, blasting is the most common and relevant impact load type. Measurements associated with pile driving have also been performed but, as commented above, they often result in low vibration velocities, which in most cases are harmless to young concrete. However, for both of these load types the soil or ground properties are of great importance for the vibration propagation, from source of vibration towards concrete construction. Field experiments and observations with direct impacts against the concrete are not documented, except for certain types of tests to determine the energy absorption capacity, but these have been excluded here. No field measurements have been carried out within the project but results from previous and related projects were used to obtain relevant load data, to verify the analytical models and to conduct comparisons of results. In these cases the acceleration measurements were done during blasting in tunnels through hard rock, see Sections 1.4. When it comes to testing in laboratory environments, it is not practical to use explosives but traditionally vibratory loads have been produced by using a shaking table that provides long-lasting continuous vibration or impact loads from pendulum hammers or similar.

6.3 Concrete and shotcrete

The two cases of shotcrete on hard rock exposed to blasting and cast laboratory specimens subjected to direct impact loads have been presented in a doctorate thesis [9] using finite element models. Stress wave propagation is described in the same way whether it is through hard rock towards a shotcrete lining or through a constructional element of young concrete. However, the failure modes differ for the two cases where shotcrete usually is damaged through loss of bond, partly or over larger sections that may result in shotcrete falling down. Cracking in shotcrete is unusual and has not been observed during previous in situ tests, see Section 1.4. For this reason, it is concluded that cracking of shotcrete need not be described in the numerical analyses and that elastic material models may be used, which has also been shown to give good conformity with in situ test results, see [2 and 6]. Because of the often symmetrical geometry of tunnels, the models can be implemented in 2D and thereby effectively when sections of the rock is included, also described as an elastic material. The observation plane can be positioned vertically for a study of a tunnel profile or horizontally to see the stress distributions along the walls of tunnels or caverns. As shown in the presented examples, crack formations closest to a rock surface exposed to blasting can be accounted for and so also damping during wave propagation through the rock. The latter gives a reduction in vibration velocity with increasing distance from the detonation point while rock cracks has a filtering effect on the frequency

content. The main advantage here is that with the 2D geometry and elastic material behaviour, the model can effectively be implemented for whole tunnel sections that allows a representation of stress distributions that also includes reflections and superposition effects at sharp edges and corners. The model can thus provide a complete displacement field that includes the passage of P and S waves, and Rayleigh waves.

The shotcrete is to be seen as a relatively thin shell attached to a surface where wave propagation, reflection and superposition interact. The application of the load can be described by the three cases discussed in Section 2.4, where shotcrete on rock can be categorized as aboveground concrete while the prism case is more similar to the case of underground concrete where the impact load directly affects the concrete volume. Both types of concrete structures should however have been considered as mass concrete since they are reached by propagating stress waves. In the third case, structural concrete, it is the dynamic properties and resonance phenomena that interact with the ground motion. When damage occurs in the prisms exposed to impact loading, cracking takes place. According to the numerical examples that have been investigated in the doctorate thesis [9], it is concluded that the free vibration modes of the prism interact, resulting in large stresses at some sections where cracks may be located. This is affected by the boundary conditions of the impacted element where a completely free element such as the prism will show cracks within the middle third along its length, in this case caused by the dominate fourth vibration mode, [3]. Although this can be calculated with an elastic material model, as in the case of shotcrete, cracking and crack propagation must be described by non-linear concrete material models.

Vibration sensitivity of cast concrete and shotcrete has different critical ages because of the set accelerators used in the latter. Differences in temperature and humidity also play an important role for the cement hydration speed. When analysing the different cases the input in form of material parameters must reflect this, and preferably be based on in situ or laboratory testing. It is therefore not appropriate to e.g. use material data from testing of cast specimens in an analysis of vibration sensitivity of young shotcrete. The difference should also be considered when guidelines and recommendations are compiled, see Chapter 5. Mainly, the vibration resistance at early age is larger for a shotcrete lining than for a concrete volume extending in all three dimensions. An important factor is here the inertial forces that develop when concrete masses are accelerated by vibrations. Since the critical material property of shotcrete is the bond to the rock and its mass per unit area is low, the inertial forces become relatively small and the vibration resistance greater compared with a more homogeneous concrete volume. In the latter case, a concrete element can be pulled apart upon passage of stress waves with cracking as a result. The dimensions of a concrete element in relation to the wavelength are also important with respect to reflection, superposition and build-up of stresses. Within a thin shotcrete lining, large stresses will not accumulate to the same extent as in an element with a length that is ten times longer or more.

Bibliography

- [1]. ACI Committee 116. Cement and concrete terminology, ACI 116R-90. Detroit, MI: American Concrete Institute; 1990.
- [2]. Ahmed L, Ansell A, Malm R. Finite element simulation of shotcrete exposed to underground explosions. *Nordic Concrete Research* 45:59-74, 2012.
- [3]. Ahmed L, Ansell A, Malm R. Numerical modelling and evaluation of laboratory tests with impact loaded young concrete prisms. Submitted to *Materials and Structures*, 2015.
- [4]. Ahmed L, Ansell A. Laboratory investigation of stress waves in young shotcrete on rock. *Magazine of Concrete Research* 64(10):899-908, 2012.
- [5]. Ahmed L, Ansell A. Structural dynamic and stress wave models for the analysis of shotcrete on rock exposed to blasting. *Engineering structures* 35:11-17, 2012.
- [6]. Ahmed L, Ansell A. Vibration vulnerability of shotcrete on tunnel walls during construction blasting. *Tunnelling and Underground Space Technology* 42:105–111, 2014.
- [7]. Ahmed L. Laboratory simulation of blasting induced bond failure between rock and shotcrete. Stockholm: Rock Engineering Research Foundation. BeFo report 116, 2012.
- [8]. Ahmed L. Models for analysis of shotcrete on rock exposed to blasting. Licentiate thesis. Stockholm: KTH Royal Institute of Technology; 2012.
- [9]. Ahmed L. Models for analysis of young cast and sprayed concrete subjected to impact-type loads. Doctorate thesis. Stockholm: KTH Royal Institute of Technology; 2015.
- [10]. Akins KP, Dixon DE. ACI SP-60-Concrete Structures and construction vibrations. Detroit, MI: American Concrete Institute; 1979,
- [11]. Ansell A, Ahmed L. Impact load vibrations on young concrete. Submitted to *Structural Concrete*, 2015.
- [12]. Ansell A, Silfwerbrand J. The vibration resistance of young and early age concrete. *Structural Concrete* 4(3):125–134, 2003.
- [13]. Ansell A. Dynamically loaded rock reinforcement. Doctoral thesis. Stockholm: KTH Royal Institute of Technology; 1999.
- [14]. Ansell A. A Literature review on the shear capacity of dynamically loaded concrete structures. Stockholm: KTH Royal Institute of Technology, Concrete Structures. Report 89, 2005.

- [15]. Ansell A. A Literature review on the vibration resistance of young and early age concrete. Stockholm: KTH Royal Institute of Technology, Concrete Structures. Report 68, 2002.
- [16]. Ansell A. Dynamic finite element analysis of young shotcrete in rock tunnels. *ACI Structural Journal* 104(1):84-92, 2007.
- [17]. Ansell A. In situ testing of young shotcrete subjected to vibrations from blasting. *Tunnelling and Underground Space Technology* 19(6):587-596, 2004.
- [18]. Ansell A. Recommendations for shotcrete on rock subjected to blasting vibrations, based on finite element dynamic analysis. *Magazine of Concrete Research* 57(3):123-133, 2005.
- [19]. Ansell A. Shotcrete on rock exposed to large-scale blasting. *Magazine of Concrete Research* 59(9):663-671, 2007.
- [20]. Assessing vibration- A technical guideline. Sydney: NSW Department of Environment and Conservation; 2006.
- [21]. Aure TW, Ioannides AM. Numerical analysis of fracture process in pavement slabs. *Canadian Journal of Civil Engineering* 39(5):506-514, 2012.
- [22]. Bastian CE. The effect of vibrations on freshly poured concrete. *Foundation Facts* 6(1):14-17, 1970.
- [23]. Bischoff PH, Perry SH. Compressive behaviour of concrete at high strain rates. *Materials and Structures* 24(6):425-450, 1991.
- [24]. Bro2004. Swedish Road Administration (in Swedish). Borlänge: Vägverket, Publ 2004:56; 2004.
- [25]. Bryne L-E. Time dependent material properties of shotcrete. Doctoral thesis. Stockholm: KTH Royal Institute of Technology; 2014.
- [26]. Byfors J. Plain concrete at early ages. Stockholm: Swedish Cement and Concrete Institute; 1980.
- [27]. Dowding CH. Construction vibrations. Upper Saddle River, NJ: Prentice-Hall; 1996.
- [28]. Esteves JM. Control of vibration caused by blasting. Lisbon: Laboratorio de Engenharia Civil; 1978.
- [29]. Goel MD, Matsagar VA. Blast-resistant design of structures. *Practice Periodical on Structural Design and Construction* 19(2):1-9, 2014.
- [30]. Heiniö M. Rock excavation handbook. Helsinki: Sandvik Tamrock Corp; 1999.
- [31]. Hulshizer AJ, Desai AJ. Shock vibration effects on freshly placed concrete. *Journal of Construction Engineering and Management* 110 (2):266-285, 1984.
- [32]. Hulshizer AJ. Acceptable shock and vibration limits for freshly placed and maturing concrete. *ACI Material Journal* 93(6):524-533, 1996.
- [33]. International Federation for Structural Concrete. *fib Model code for concrete structures 2010*. Lausanne: Wilhelm Ernst & Sohn, 2013.
- [34]. Issa MA. Investigation of cracking in concrete bridge decks at early ages. *Journal of Bridge Engineering* 4(2):116-24, 2003.
- [35]. James G. Modelling of young shotcrete on rock subjected to shock wave. Master thesis. Stockholm: KTH Royal Institute of Technology; 1998.

- [36]. Kendorski FS, Jude CV, Duncan WM. Effect of blasting on shotcrete drift linings. *Mining Engineering* 25(12):38-41, 1973.
- [37]. Krell WC. The effect of coal mill vibration of fresh concrete. *Concrete International* 1(12):31-34, 1979.
- [38]. Kwan AKH, Lee PKK. A study of the effects of blasting vibration on green concrete. Hong Kong: Geotechnical Engineering Office, The government of the Hong Kong special administrative region. Geo Report No. 102, 2000.
- [39]. Kwan AKH, Zheng W, Lee PKK. Shock vibration test of concrete. *ACI Material Journal* 99(4):361-370, 2002.
- [40]. Kwan AKH, Zheng W, Ng IYT. Effects of shock vibration on concrete. *ACI Material Journal* 102(6):405-413, 2005.
- [41]. Leppänen J. Concrete structures subjected to fragment impacts - Dynamic behaviour and material modelling. Doctoral thesis. Gothenburg: Chalmers University of Technology; 2004.
- [42]. Magnusson J. Structural concrete elements subjected to air blast loading. Licentiate thesis. Stockholm: KTH Royal Institute of Technology; 2007.
- [43]. Malvar LJ, Crawford JE. Dynamic increase factors for concrete. Proceedings of the 28th DoD Explosives Safety Seminar Held in Orlando. Orlando, FL: Naval Facilities Engineering Service Centre; 1998.
- [44]. Muller-Rochhotz JFW. Traffic vibration of a bridge deck and hardening of lightweight concrete. *Concrete International* 8(11):23-26, 1986.
- [45]. Nakano N, Okada S, Furukawa K, Nakagawa K. Vibration and cracking of tunnel lining due to adjacent blasting (in Japanese, Abstract in English). Proceedings of the Japan Society of Civil Engineers. Rombun-Hokokushu; 1993.
- [46]. Neville AM. Properties of concrete. London: Prentice-Hall; 2010
- [47]. Nyström U. Modelling of concrete structures subjected to blast and fragment loading. Doctoral thesis. Gothenburg: Chalmers University of Technology; 2013.
- [48]. Olofsson SO. Applied explosives technology for construction and mining. Sweden: Applex, Ärla; 1988.
- [49]. Oriard LL, Coulson J H. TVA blast vibration criteria for mass concrete. Proceeding Conference of ASCE. Portland, OR: Preprint; 1980.
- [50]. Persson P-A. The Relationship between Strain Energy, rock Damage, fragmentation, and throw in rock blasting. *Fragblast - International Journal of Blasting and Fragmentation* 1(1):99-110, 1997.
- [51]. Reidarman L, Nyberg U. Blast vibrations in the Southern Link tunnel - Importance for fresh shotcrete? (in Swedish: Vibrationer bakom front vid tunneldrivning i Södra Länken - Betydelse för nysprutad betong?). Stockholm: Rock Engineering Research Foundation. SveBeFo-report 51, 2000.
- [52]. Reinhardt HW. Concrete under impact loading, tensile strength and bond. *Heron* 27(3) Delft University of Technology, the Netherlands, 1982.
- [53]. Revey GF. Managing rock blasting work in urban environments. *Practice Periodical on Structural Design and Construction* 11(2): 86-92, 2006.
- [54]. Simulia, Abaqus user's examples and theory manual, version 6.12.

- [55]. Simulia: < http://www.simulia.com/products/abaqus_explicit.html >; 2014.
- [56]. Siwula J, Helwany S, Richard L. Construction vibration attenuation with distance and its effect on the quality of early age concrete. Milwaukee: Wisconsin Highway Research Program. Report WHRP 11-02, 2011.
- [57]. Swedish Concrete Handbook. Betonghandbok–Material. Stockholm: AB Svensk Byggtjänst; 1994.
- [58]. Tunnel 99. Swedish Road Administration (in Swedish). Borlänge: Vägverket Publ 1999:138; 1999.
- [59]. Wood DF, Tannant DD. Blast damage to steel fibre reinforced shotcrete. In: Fibre-reinforced Concrete – Modern Developments. Vancouver: University of British Columbia UBC Press, 1994.

BeFo



Box 5501
SE-114 85 Stockholm

info@befoonline.org • www.befoonline.org
Visiting address: Storgatan 19

ISSN 1104-1773